Budapest University of Technology and Economics (BME)
Faculty of Electrical Engineering and Informatics (VIK)

Proof of the influence of the Tensor Product model representation on the feasibility of Linear Matrix Inequality

---

Scientific Student Conference Paper

Author: Alexandra Szöllősi, electrical engineering MSc. student
Budapest University of Technology and Economics (BME)
Faculty of Electrical Engineering and Informatics (VIK)

Supervisor: Péter Zoltán Baranyi, D.Sc.
Budapest University of Technology and Economics (BME)
Faculty of Electrical Engineering and Informatics (VIK)

2014

Contents

Abstract

Modern quasi Linear Parameter Varying (qLPV) state-space model and Linear Matrix Inequality (LMI) based multi-objective convex optimization aimed control theories and design methods can be basically divided into three steps:

i) identification of the qLPV state-space model

ii) derivation of the polytopic representation from the qLPV model

iii) substitution of the polytopic representation into LMI based control design methods in order to attain the controller and observer system components

The main focus in the scientific research initiatives was mostly on step *iii*, addressing the investigation and manipulation of LMIs to attain the optimized controller and observer performance, which achieved a significant literature. Moreover, the current widely accepted standpoint among scientific research is represented by the statement that the LMI based control design methods give an optimal solution on the identified qLPV model. However, step *ii*, the effect of the procedure deriving the polytopic model and its effect on the LMI based control design methods was given less attention. A hypothesis published in 2009 discusses and points out this fact that beside the procedure deriving the manipulation of the polytopic representation in step *ii* is necessary and has relatively the same extent of significance as step *iii*, namely the fact that the LMI based control design methods do not give an optimal solution on the identified qLPV model but rather on the polytopic representation at hand and the polytopic manipulation therefore leads to further potential optimization possibilities with a relatively similar importance as the LMI based control design methods.

Goals

In this context the aim of the Scientific Student Conference paper is to systematically investigate and prove the above mentioned - so far unconfirmed - hypothesis both for the control and observer design combined with various polytopic manipulation techniques. As a consequence this proof declares the necessity hence the

importance of the polytopic manipulation. In addition a further aim is to show that the manipulation plays an important role in deriving the optimal solution, since the polytopic representation is not invariant. The proof of the hypothesis and the regarding concepts gain further new research directions in the field of qLPV and LMI based control theory research.

Methodology

In order to achieve the above specified goals the paper presents the systematic method which was developed and executed for investigating the hypothesis, its results and consequences which lead to the proof of the hypothesis. The investigation includes the main factors of the polytopic representation influencing the feasibility regions of the LMI based control design, specifically *i)* the manipulation of the vertexes' position and *ii)* the size and complexity of the representation, i.e. the number of the vertexes contained in the TP model type polytopic representation. The proof is based on a complex control design example, where the influence of these factors can be clearly indicated. Furthermore the paper shows via the example that the maximal achievable parameter space of the controller and observer also depend from these factors. The example model consists of the complex Nonlinear Aeroelastic Test Apparatus (NATA) model of the three Degree of Freedom (3-DoF) aeroelastic wing section including Stribeck friction. The methodology is based on the Tensor Product (TP) model transformation based Control Design Framework that supports the flexible manipulation of these factors.

Literature references

To discuss the significant paradigm changes described in the preliminaries of the introduction regarding the mathematical, control theory and system modeling and identification advancements, the paper cites essential publications from the last 100 years. Concerning the mathematical and control theory formalisms and concepts utilized in the paper are source to literature of the last 15 years. Lastly, papers in the reference list published between 2009 and 2014 directly lead to the fundamentals of the specified goals.

Results and the formulated statement of the Scientific Student Conference paper

Based on the systematical investigation and results the Scientific Student Conference paper presents a TP model transformation based solution to prove the hypothesis

via the following statements:

The manipulation of the polytopic TP model representation's Linear Time Invariant (LTI) vertexes influence the feasibility of LMI based control design methods:

i) The position of the LTI vertexes, defining the convex hull of the TP model type polytopic representation influence the feasibility of LMI based control design.

ii) The complexity of the TP model, namely the number of the LTI vertexes contained in the TP model also influence the feasibility of LMI based control design.

iii) Statement *i)* and *ii)* is valid both for the design of the controller and observer system elements but the influence differs from each other, in fact in certain cases it influences in an opposite way. This may raise further optimization questions: since so far the controller and observer have been designed on the same polytopic representation a design with separate TP model type polytopic representations may induce further benefits.

iv) The position and number of the LTI vertexes of the polytopic TP model representation also influence the size of the achievable parameter space of the feasible design.

Some details of the statements and the proving results described in the paper have been presented in the following publications:

- A. Szöllősi, P. Baranyi: Influence of Complexity Relaxation and Convex Hull Manipulation on LMI based Control Design, Proceedings of the 9th IEEE International Symposium on Applied Computational Intelligence and Informatics (SACI), pp. 145-151., 2014.

- A. Szöllősi, P. Baranyi, P. Várlaki: Example for Convex Hull Tightening increasing the feasible parameter region at Linear Matrix Inequality based Control Design, Proceedings of the 18th IEEE International Conference on Intelligent Engineering Systems (INES), pp. 175-180., 2014.

Also, the aspects of the above mentioned statement and proof have been formulated into a comprehensive study which has been submitted to the Asian Journal of Control international scientific journal (impactfactor: 1.411) for publication.

Budapest, 2014

Structure of the Scientific Student Conference paper

The Scientific Student Conference paper consists of three main parts: the introduction in Chapter 1 presents the preliminaries, background and a general overview which leads to the motivation and goals of the paper. Next, the statement formulated by the author is described in Chapter 2, which is followed by the proof of the statement in Chapter 3 and 4, containing the theory of the proposed methodology and its application resulting in the proving results. Finally, the paper is closed with the conclusion in Chapter 5, and an appendix containing the acronyms is attached.

Chapter 1

Introduction

The introduction consists of two main parts: Section 1.1 presents the preliminaries and a general overview describing the important conceptual changes which lead to the specific objectives of the Scientific Student Conference paper and Section 1.2 describes the mathematical notations and methods, which will be applied throughout the paper.

1.1 Preliminaries and general overview

The Scientific Student Conference paper addresses a topic in connection with the significant paradigm and conceptual changes in the last decades subject to modern nonlinear and multi-objective control theory and its associated mathematical concepts described in Section 1.1.1 and system identification theory described in Section 1.1.2. These conceptual changes significantly differ from each other in their concepts although these fields are closely related, and in most cases are even consecutive steps following each other sequentially. The difference generates a representational and formalism gap which makes the sequential application of identification tools with the control theory apparatus difficult to accomplish. A possible resolving tran-

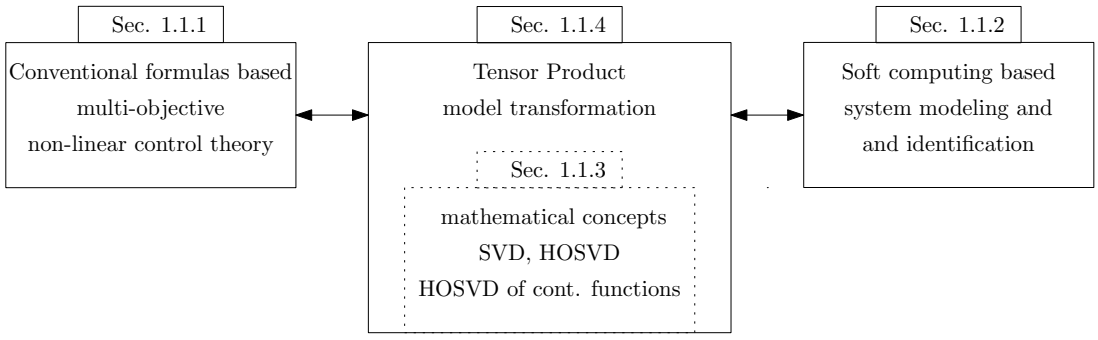

Figure 1.1: *General overview*

sition has been the subject of several studies in recent years, a connection would require an appropriate conversion and a uniform representation. Such a possible connection and transition can be represented by the Tensor Product (TP) model transformation and the finite element Tensor Product type polytopic model representation. Its mathematical preliminaries will be described in Section 1.1.3 and the TP model transformation itself, enabling the connection between the significant conceptual changes will be illustrated in Section 1.1.4.

1.1.1 Multi-objective nonlinear control theory

The modeling and control of nonlinear systems with multiple objectives is a current challenge in engineering in the present day. One commonly accepted approach is represented by quasi Linear Parameter Varying (qLPV) modeling and Linear Matrix Inequality (LMI) based design techniques.

Nonlinear modeling through qLPV models

The qLPV representation of a model has the ability to describe nonlinear systems. This is achieved through a Linear Time Invariant (LTI) state-space model where the system matrix $\mathbf{S}(\mathbf{p})$ incorporates a parameter variance through the vector $\mathbf{p}$, which can contain both internal - e.g. elements of the state vector - and external dependencies. The parameter variance can hold both continuous functions $\mathbf{p}_{1,2,\ldots}(t)$ or discrete state variables $\mathbf{p}_{1,2,\ldots}[k]$ as elements. The theory of qLPV system representations appeared in connection with aerospace control where the representation describes a systematical approach to gain scheduling control for nonlinear systems [1] in 1991. Further advances extended the topic of qLPV systems such as passivity and H_∞ theories, robust adaptive control [2], switching control systems [3] and intelligent control [4, 5] through the 2000s. The method of qLPV representation can be applied to a wide range of problems and applications.

Multi-objective control design theories through LMIs

In addition modern LMI based controller and observer design methods have the ability to efficiently handle the controller and observer design process expanding also the possibilities with multi-objective requirements, e.g. constraints such as overshoot constraint, settling time constraint, etc. This makes this numerical computation based method also for a wide range of problems and applications effective. This new approach was established and elaborated through the efforts of Gahinet, Balas, Chilai, Boyd, and Apkarian [6, 7, 8, 9, 10] during the 1990s and the geometrical representation of convex optimization was introduced by József Bokor [11]. Also,

the solution (feasibility) of LMIs can be reinterpreted as a convex optimization problem. Simultaneously efficient numerical mathematical methods and algorithms were developed for solving the convex optimization problems for LMIs [12].

The topics of qLPV models and theit polytopic representation based LMI convex optimization methods are expanding to a rich literature of control theory to the present day.

1.1.2 System modeling and identification theory

David Hilbert gave a speech at the Paris Conference of the International Congress of Mathematicians in 1900, where he presented 23 hypotheses regarding unsolved mathematical problems [13, 14, 15, 16]. He assumed these hypotheses would be the unanswered issues of the 20th century. The 13th hypothesis states that continuous multi-variable functions would exist which could not be decomposed as a finite superposition of continuous functions of a smaller number of variables. This statement was proven false in 1957 by V. I. Arnold [17]. Also, a general representation theorem with an attached proof was developed by the mathematician Kolmogorov in the same year which allows a decomposition of continuous multi-variable functions into one-dimensional functions [18], see also [19] and [20]. Kolmogorov's proof was a legitimate evidence for the existence of universal approximators, which induced further research: during the last decades it has been proven that the different concepts of neural networks, genetic algorithms and fuzzy logic systems exist as universal approximator systems [20, 21, 22, 23, 24]. Thus soon these concepts proved to be effective applied theories in system modeling and identification theory extending the possibilities besides the conventional theorems of e.g. black-box identification, engineering considerations etc.

These identification concepts and the powerful control design and optimization techniques described previously in Section 1.1.1 significantly differ in their concept and mathematical representations. Neural networks are basically graphs with a set of connections and the weights of these interconnections, fuzzy logic is basically a database of linguistic rules equipped with an inference technique and evolutionary algorithms are basically algorithms, which are all rather far from analytic closed-form expressions applied in LMI based control theory.

1.1.3 Mathematical advancements

In order to connect the significant paradigm and conceptual changes subject to modern multi-objective nonlinear control theory and system modeling and identification theory the mathematical concepts will be described in this section including the re-

cent advancements in multi-linear algebra concerning Singular Value Decomposition (SVD) and Higher-Order Singular Value Decomposition (HOSVD) followed by the concept of the decomposition of continuous functions through HOSVD and the TP model transformation as the overall uniting concept.

Multi-linear algebra concerning SVD and HOSVD

A generalized method for matrix diagonalization and component separation is represented by the Singular Value Decomposition (SVD): it represents a concept, where a general matrix is diagonalized through decomposing it into a diagonal matrix containing the main components (singular values) and two orthonormal bases. The history of SVD dates back to the 1850s [25] and the elaboration was presented by Golub in 1965 and the 1970s [26, 27, 28]. SVD gained popularity in various scientific fields [29, 30, 31, 32, 33] from signal processing, image processing, statistics, etc. Regarding the advancements in computing technology through the decades the improvements made the addressing of large scale multi-dimensional problems possible, which lead to a further generalization: the Higher-Order Singular Value Decomposition (HOSVD) or multi-dimensional SVD published in 2000 by Lieven De Lathauwer [34] can decompose also a general, but N-dimensional tensor into also a matrix containing the main, higher order components (higher order singular values) and an orthonormal basis system. This is attained in L_2 norm. In summary, HOSVD has the ability to determine the structure and the significance of each contained component of a given tensor. The first event where HOSVD was handled as a key topic was the Workshop on Tensor Decompositions and Applications held in Luminy, Marseille, France, in 2005. Implicitly HOSVD and its concepts has been formulated and presented also in fuzzy approximation [35, 36] during the 1990s and as independent component analysis (ICA) in [37], as well as dimension reduction for higher-order factor analysis-type problems to decrease computational complexity in [38] also during the 1990s.

HOSVD of multi-variable continuous functions and Tensor Product model transformation

Following the publication of HOSVD soon the definition of HOSVD for multi-variable continuous functions and the associating definition of rank regarding the importance and contribution of the corresponding variables has been presented in 2006 [39, 40, 41]. Similar to HOSVD, the HOSVD for multi-variable continuous functions constructs a higher order ranking of products consisting of orthonormal weighting function systems for each in the function included variables. These weighting functions are the singular functions similar to the singular matrices and vectors in

SVD and HOSVD. Similarly the same way the higher order singular values indicate the importance, contribution and rank of each associated singular vector product in Frobenius norm in case of HOSVD, the singular values in case of HOSVD of continuous functions also indicate these attributes for the singular functions through the continuous variant of the Frobenius norm. In summary the HOSVD of continuous functions inherits many attributes from HOSVD. In this context the application is performed also in a similar sense, e.g. main component analysis, noise filtering, trade-off between complexity and accuracy, etc.

The TP model transformation introduced in 2006 [42, 43, 44, 45] is a numerically executable method which is able to convert a model given through a set of continuous functions into a set of TP functions by reconstructing the HOSVD of the continuous functions [40]. The TP model transformation also inherits many attributes from HOSVD which reflects on its features: it has the ability to determine the fundamental structure and the significance of each component contained in the set of TP functions. The TP model transformation has been extended with different convex manipulation techniques to be able to generate convex variants of the TP function. These convex manipulation techniques enable the possibility to construct a convex combination, which consists of the combination of the elements of the core tensor (termed as vertexes) and the one variable weighting function products. This convex combination forms thereby a geometric polytopic structure, which is defined through its vertex points. The TP model transformation and the convex manipulation will be detailed in the next section.

1.1.4 The Tensor Product model transformation connecting the different concepts and representations

As previously described in Section 1.1.2, identification techniques based on soft-computing concepts can prove to be effective approaches considering system modeling and identification problems throughout different engineering fields, particularly in such circumstances where formulating the model through analytic closed form formulas - e.g. through physical or engineering considerations - would seem difficult. As a consequence a number of identification methods have appeared and spread: e.g. neural networks, fuzzy theory, genetic algorithms, etc. However, due to the conceptual differences in structure and representation, which may also prove to be problem-dependent, it is difficult to continue with the control system design theories described in Section 1.1.1.

In this context the construction of TP models is motivated by the fact that commonly applied and well developed frameworks and design techniques exist to find the efficient solutions to engineering problems, which are compatible with the struc-

ture of TP models. This enables that the modern polytopic and LMI based control theories can be basically directly applied on TP models. As previously described in Section 1.1.3 the mathematical conversion to attain TP models is accomplished through the TP model transformation which reconstructs the HOSVD of continuous functions and the uniform representation is established through the finite element TP type polytopic model representation (TP model).

In addition it is also worth mentioning that measurement based identification methods or identification through engineering and physical considerations - excluding some special cases - may contain significantly larger errors (in many cases the relatively small, but non-zero singular values may represent a distorting noise in the system) in their results than the model attained through the TP model transformation. There may exist cases, where a given model does not possesses an exact TP model, however it can be still approximated, even with still a smaller scale error than that resulting of the identification. Therefore, executing the TP model transformation and validating the resulting TP model could be more beneficial than identification. In cases, where the identification contains efficient methods, it still may be beneficial to execute a conversion to the TP model and validating it instead of the identified model, since the TP model still incorporates relatively smaller errors of a given model instead of the identified model, or even none if there exists an exact TP model. In summary, it can be concluded, that the TP model transformation could be a last step of identification and as a general interface, a preprocessing step for control design.

The TP model transformation includes the following features:

- The TP model transformation can be executed irrespective to the form of the initial model, which can be given through analytic closed-form expressions, neural networks, fuzzy logic, etc., the only requirement consists of the fact that the identified model has to be able to be discretized over a grid.
- If the TP model representation exist, the transformation generates the exact TP model representation of the given model. If the TP model representation does not exist, an approximate representation of the model is derived.
- The TP model transformation numerically constructs the HOSVD based TP model form of a given qLPV model [39, 40, 41] with the following attributes:
  - The multi-variable continuous functions result in products consisting of orthonormal one-variable weighting function systems.

  - The number of LTI vertexes, which determine the fundamental structure and the significance of each component are minimized.
  - The LTI vertexes are constructed into an orthogonal basis system.
  - The LTI vertexes and weighting function systems are constructed into a higher order ranking corresponding to the significance of each component.

- Based on component analysis indicating the importance and contribution of each corresponding LTI vertex component a trade-off between complexity and accuracy in L_2 norm [46, 47] is also featured. Through disposing the components which hold a small extent of contribution a complexity decrease at the expense of accuracy is possible, and vice versa.

- The TP model transformation is also able to generate different convex TP model representations, therefore different polytopic representations of a same given model. The polytopic representation given its structure is directly executable with LMI based control design theorems.

1.2 The mathematical notations and methods applied in the paper

In this Section the mathematical notations and methods applied in the Scientific Student Conference paper will be recalled from source [42]. Since the Scientific Student Conference paper's investigations are subject to a control design example of a given qLPV model, the applied mathematical notations and methods will be therefore described in its accordance.

Notations

The following notations are used within this paper:

$n = 1 \dots N$	index values, the upper bound is denoted through a capital letter
$\Omega = \omega_1 \times \cdots \times \omega_N$	parameter space defined through each dimension $n = 1 \dots N$
$G = G_1 \times \ldots \times G_N$	discretization grid defined through each dimension $n = 1 \dots N$
$a, b, \dots$	scalar values
$\mathbf{a}, \mathbf{b}, \dots$	vectors
$\mathbf{A}, \mathbf{B}, \dots$	matrices
$\mathcal{A}, \mathcal{B}, \dots$	tensors
$\mathcal{F}^{D(\Omega,G)}$	tensor containing the discretized variant of function $f(x)$ over Ω and G
$\mathfrak{V}, \mathfrak{W}, \dots$	matrix containing the discretized variant of $f(x)$
$\mathcal{A} \times_n \mathbf{U}_n$	tensor multiplication along dimension n with matrix $\mathbf{U}_n$
$\mathcal{A} \times_1 \mathbf{U}_1 \cdots \times_N \mathbf{U}_N$	tensor multiplication along dimension $1 \dots N$ with matrices $\mathbf{U}_1 \dots \mathbf{U}_n$
$\mathcal{A} \bigboxtimes_{n=1}^{N} \mathbf{U}_n$	compact tensor multiplication interpreting $\mathcal{A} \times_1 \mathbf{U}_1 \cdots \times_N \mathbf{U}_N$

$\mathcal{A} \underset{n \in N}{\boxtimes} \mathbf{U}_n$	equivalent compact tensor multiplication notation, $N : \{1 \dots N\}$
$R_n = rank_n()$	rank of tensor along the n-th dimension

qLPV model

Assume a state-space model is given with $\mathbf{u}(t) \in \mathbb{R}^K$ input, $\mathbf{y}(t) \in \mathbb{R}^L$ output, $\mathbf{x}(t) \in \mathbb{R}^M$ state vector, $\mathbf{p}(t) \in \Omega \subset \mathbb{R}^N$ parameter vector with dimension N, parameter space $\Omega = \omega_1 \times \cdots \times \omega_N$ along each dimension $n = 1 \dots N$ and system matrix $\mathbf{S}(\mathbf{p}(t)) \in \mathbb{R}^{(M+K=O)\times(M+L=I)}$:

$$\begin{pmatrix} \dot{\mathbf{x}}(t) \\ \mathbf{y}(t) \end{pmatrix} = \mathbf{S}(\mathbf{p}(t)) \begin{pmatrix} \mathbf{x}(t) \\ \mathbf{u}(t) \end{pmatrix}. \tag{1.1}$$

where the system matrix $\mathbf{S}(\mathbf{p}(t))$ is:

$$\mathbf{S}(\mathbf{p}(t)) = \begin{pmatrix} \mathbf{A}(\mathbf{p}(t)) & \mathbf{B}(\mathbf{p}(t)) \\ \mathbf{C}(\mathbf{p}(t)) & \mathbf{D}(\mathbf{p}(t)) \end{pmatrix}.$$

If the parameter vector $\mathbf{p}(t)$ includes elements of the state vector $\mathbf{x}(t)$, the system belongs to the class of nonlinear qLPV models. In contrast, if the parameter vector $\mathbf{p}(t)$ does not include elements of the state vector $\mathbf{x}(t)$, then the model belongs to the class of LPV systems.

Finite element Tensor Product type polytopic model representation - Tensor Product model representation

The TP model transformation converts a model given through a set of functions, in case of qLPV models through the system matrix $\mathbf{S}(\mathbf{p}(t))$ from equation (1.1) for any parameter $\mathbf{p}(t)$ into the finite element Tensor Product type polytopic model

$$\begin{aligned} \mathbf{S}(\mathbf{p}(t)) &= \sum_{i_1=1}^{I_1} \sum_{i_2=1}^{I_2} \cdots \sum_{i_N=1}^{I_N} w_{n,i_n}(p_n(t)) \mathbf{S}_{i_1,i_2,\dots,i_N} = \\ &= \mathcal{S} \underset{n=1}{\overset{N}{\boxtimes}} \mathbf{w}_n \left(p_n \left(t \right) \right), \end{aligned} \tag{1.2}$$

which represents a parameter-dependent convex combination of linear time-invariant (LTI) system matrices, or vertex systems $\mathbf{S} \in \mathbb{R}^{O \times I}$ and weighting functions $w_n(p_n(t))$, where

$$\begin{aligned} \forall n, i, p_n(t) : \;& w_{n,i}(p_n(t)) \in [0, 1], \\ \forall n, i_n, p_n(t) : \;& \sum_{i=1}^{I_n} w_{n,i_n}(p_n(t)) = 1. \end{aligned}$$

The (N+2) dimensional coefficient of the core tensor $\mathcal{S} \in \mathbb{R}^{I_1 \times \ldots \times I_n \times O \times I}$ is constructed from the LTI vertex systems $\mathbf{S}_{i_1,\ldots,i_N}$ and the row vector $\mathbf{w}_n\left(p_n\left(t\right)\right)$ containing the one variable weighting functions $w_{n,i_n}(p_n(t))$, $i_n = 1 \ldots I_N$. Figure 1.2 illustrates a polytopic representation with the system matrix $\mathbf{S}(\mathbf{p}(t))$ of a qLPV model, vertex points $\mathbf{S}_{i_1,\ldots,i_N}$ and polytopic convex hull defined by the position of the vertexes.

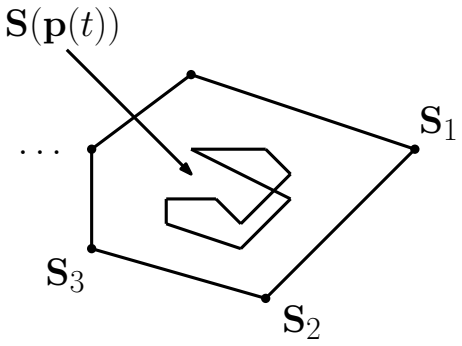

Figure 1.2: *Polytopic representation of* $\mathbf{S}(\mathbf{p}(t))$

SNNN type Tensor Product model representation

The TP model representation possess an SNNN (sum normalized, non-negative) type convex hull if its weighting functions satisfy Equation 1.3-1.4:

$$\text{SN condition:} \quad \forall n, i_n, p_n(t) : w_{n,i_n}(p_n(t)) \in [0,1] \tag{1.3}$$

$$\text{NN condition:} \quad \forall n, i_n, p_n(t) : \sum_{i=1}^{I_n} w_{n,i_n}(p_n(t)) = 1. \tag{1.4}$$

NO and CNO type Tensor Product model representation

The TP model representation possess an NO (normalized) type convex hull if its weighting functions are normalized, that is if it satisfies 1.3, 1.4, and the largest value of all weighting functions is 1. The convex TP model is a CNO (close to normal) type if it also satisfies both 1.3 and 1.4 and the largest value of all weighting functions is 1 or close to 1.

The n-mode rank of a given function

The n-mode rank of function $\mathcal{Y} = f(\mathbf{x}) \in \mathbb{R}^{O \times I}$ and $\mathbf{x} \in \Omega \subset \mathbb{R}^N$ is represented by $R_n = rank_n(\mathcal{Y}, \Omega)$. This indicates the number of non-zero singular values along the n-th dimension, therefore $R_n = rank_n(\mathcal{Y}, \Omega) = rank_n(\mathcal{S})$, where tensor $\mathcal{S}$ is derived through the HOSVD of continuous functions, namely $f(\mathbf{x}) = \mathcal{S} \overset{N}{\underset{n=1}{\boxtimes}} \mathbf{w}_n(x_n)$.

In case of qLPV models the n-mode rank of a given function is represented similarly through $R_n = rank_n(\mathbf{S}(\mathbf{p}(t)), \Omega)$, which also indicates the number of non-zero singular values included in the TP model representation along the n-th dimension, therefore $R_n = rank_n(\mathbf{S}(\mathbf{p}(t)), \Omega) = rank_n(\mathcal{S})$, where tensor $\mathcal{S}$ is derived through the HOSVD of continuous functions, namely $\mathbf{S}(\mathbf{p}(t)) = \mathcal{S} \overset{N}{\underset{n=1}{\boxtimes}} \mathbf{w}_n(p_n(t))$.

Discretization space $D(\Omega, G)$

$D(\Omega, G)$ represents the discretization space where a given model with parameter space $\Omega = \omega_1 \times \ldots \times \omega_N$ is discretized with grid $G = G_1 \times \ldots \times G_N$ along each dimension $n = 1 \ldots N$.

Discretized function

For each continuous function $\mathcal{Y} = f(\mathbf{x}) \in \mathbb{R}^{O \times I}$, $\mathbf{x} \in \Omega \subset \mathbb{R}^N$ describing a given e.g. qLPV model, tensor $\mathcal{F}^{D(\Omega,G)} \in \mathbb{R}^{G_1 \times \ldots \times G_N}$ represents the discretized variant of the function in the discretization space $D(\Omega, G)$.

Row vector $\mathbf{g}_n$ defines the - typically but not necessarily equidistant - positions of the grid as

$$\mathbf{g}_n = \begin{pmatrix} g_{n,1} = \omega_n^{min} & \cdots & g_{n,G_n} = \omega_n^{max} \end{pmatrix} \tag{1.5}$$

along each dimension $n = 1 \ldots N$. The elements $\mathcal{F}_{i_1,\ldots,i_N} \in \mathbb{R}^{O_1 \times \ldots \times O_K}$ of tensor $\mathcal{F}^{D(\Omega,G)}$ are $\mathcal{F}_{i_1,\ldots,i_N} = f(\mathbf{x})$, where vector $\mathbf{x} = \begin{pmatrix} g_{1,i_1} & \cdots & g_{N,i_N} \end{pmatrix}$.

Similarly if the row vector $\mathbf{w}(x)$ is given as

$$\mathbf{w}(x) = \begin{pmatrix} w_1(x) & \cdots & w_I(x) \end{pmatrix}, \tag{1.6}$$

incorporating the discretized variants of the weighting functions $w_i(x)$, where $i = 1, \ldots, I$.

Then matrix $\mathfrak{W}^{D(\omega,G)} \in \mathbb{R}^{G_n \times I}$ with column vectors representing the discretized variants of the weighting functions $w_i(x)$ can be defined for each dimension $n = 1 \ldots N$ as:

$$\mathfrak{W}^{D(\omega,G)} = \begin{pmatrix} (\mathfrak{w}_1^{D(\omega,G)})^T & \cdots & (\mathfrak{w}_I^{D(\omega,G)})^T \end{pmatrix}, \tag{1.7}$$

where

$$\mathfrak{w}_i^{D(\omega,G)} = \begin{pmatrix} w_i(g_1) & \cdots & w_i(g_G) \end{pmatrix}. \tag{1.8}$$

Resulting in

$$\mathfrak{W}^{D(\omega,G)} = \begin{pmatrix} w_1(g_1) & \cdots & w_I(g_1) \\ \vdots & \ddots & \vdots \\ w_1(g_G) & \cdots & w_I(g_G) \end{pmatrix}. \tag{1.9}$$

General Tensor Product model transformation

According to sources [45] assume a model given through a set of functions $\mathcal{Y}_l = f_l(\mathbf{x})$, $l = 1, \ldots, L$, where $\mathbf{x} \in \Omega \subset \mathbb{R}^N$. In case of qLPV models $f_l(\mathbf{x})$ represents the system matrix $\mathcal{S}_l(p(t))$. $\Omega = \omega_1 \times \ldots \times \omega_N$ represents the space upon which the discretization is executed with discretization grid $G = G_1 \times \ldots \times G_N$, where G_n represents the number of gridpoints through each dimension $n = 1 \ldots N$. The distinct functions may possess different dimensionality and size, therefore $\mathcal{Y} = f_l(\mathbf{x}) \in \mathbb{R}^{O_{l,1} \times \ldots \times O_{l,K_l}}$, where $k \in \{1, \ldots, K_l\} = \mathrm{K}_l$. It is irrespective what kind of functions or equations define the model, the only requirement for the TP model transformation consists of the fact that the functions have to be discretizable over the discretization space $D(\Omega, G)$ resulting in the discretized functions $\mathcal{F}_l^{D(\Omega,G)}$. The goal is to find the finite element TP type polytopic model representation in Equation 1.2.

Since the General Tensor Product model transformation incorporates the Pseudo Tensor Product model transformation [43, 44, 45] it can be assumed a set of previously derived one variable weighting functions $\mathbf{w}_d(x_d)$ for dimensions $d \in \mathrm{D} \subseteq \mathrm{N}$ are given, or their discretized variants $\mathbf{w}_h(x_h)$, where $h \in \mathrm{H} \subseteq \mathrm{N}$ in the form of $\mathfrak{W}_h^{D(\omega_h, G_h)}$ [42]. The General TP model transformation takes the following procedure:

Algorithm 1 - General Tensor Product model transformation
Assume a model $\mathcal{Y}_l = f_l(\mathbf{x}) \in \mathbb{R}^{O_{l,1} \times \ldots \times O_{l,K_l}}$, $\mathbf{x} \in \Omega \subset \mathbb{R}^N$, $k \in \{1, \ldots, K_l\} = \mathrm{K}_l$, $l = 1, \ldots, L$, $\mathbf{w}_d(x_d)$, $d \in \mathrm{D} \subseteq \mathrm{N}$, $\mathfrak{W}_h^{D(\omega_h, G_h)}$, $h \in \mathrm{H} \subseteq \mathrm{N}$, Ω *are given and* $\forall k : \mathcal{F}_l^{D(\Omega,G)}$ *exist. The General TP model transformation results in*

$$\mathcal{Y}_l = f_l(\mathbf{x}) = \mathcal{S}_l \underset{n \in \mathrm{N}}{\boxtimes} \mathbf{w}_n(x_n). \tag{1.10}$$

- **STEP 1: Discretization**
  - *Determine tensor* $\mathcal{F}_l^{D(\Omega,G)}$ *and matrix* $\mathfrak{W}_d^{D(\omega_d, G_d)} \in \mathbb{R}^{G_d \times I_d}$.
  - *Reorder the elements of tensor* $\mathcal{F}_l^{D(\Omega,G)} \in \mathbb{R}^{O_{l,1} \times \ldots \times O_{l,K}}$ *into vectors* $\mathbf{f}_{l,j_1,\ldots,j_N} \in \mathbb{R}^{1 \times O_{l,1} O_{l,2} \ldots O_{l,K_l}}$.
  - *Compose elements* $\mathbf{m}_{j_1,\ldots,j_N} = \begin{pmatrix} \mathbf{f}_{1,j_1,\ldots,j_N} & \ldots & \mathbf{f}_{L,j_1,\ldots,j_N} \end{pmatrix}$ *which will be incorporated into tensor* $\mathcal{M}$.
- **STEP 2: Construction of the Tensor Product structure**
  - *Incorporate the previously derived weighting functions or their discretized variants* $\mathfrak{W}_d^{D(\omega_d, G_d)}$

$$\mathcal{S}' = \left(\mathcal{M} \underset{d \in D}{\boxtimes} \left(\mathfrak{W}_d^{D(\omega_d, G_d)} \right)^+ \right) \underset{h \in H}{\boxtimes} \left(\mathfrak{W}_h^{D(\omega_h, G_h)} \right)^+. \tag{1.11}$$

– *Execute Compact HOSVD (CHOSVD) by disposing all zero singular values, for each dimension* $n = 1 \dots N$*, where* $n \notin D \cup H$ *of* $\mathcal{S}'$*:*

$$\mathcal{S}' = \mathcal{S}'' \underset{n \in N, n \notin D \cup H}{\boxtimes} \mathbf{U}_n. \tag{1.12}$$

– *Denoting matrix* $\mathfrak{W}_n^{D(\omega_n, G_n)} = \mathbf{U}_n$*, where also* $n \in N, n \notin D \cup H$*. The structure of the TP model representation results in:*

$$\mathcal{M} = \mathcal{S}'' \underset{n \in N}{\boxtimes} \mathfrak{W}_n^{D(\omega_n, G_n)}. \tag{1.13}$$

– *Tensor* $\mathcal{S}''$ *can be partitioned along the* $N+1$*-th dimension in accordance to the length of vectors* $\mathbf{f}_{l, j_1, \dots, j_N}$*. Reordering the* $j_1, \dots, j_N$*-th vectors into* $O_{l,1} \times \times \dots \times O_{l,K_l}$*, and incorporating these elements into tensor* $\mathcal{S}_l$ *opposite to Step 1, tensor* $\mathcal{F}_l^{D(\Omega, G)}$ *results in:*

$$\mathcal{F}_l^{D(\Omega, G)} = \mathcal{S}_l \underset{n \in N}{\boxtimes} \mathfrak{W}_n^{D(\omega_n, G_n)}. \tag{1.14}$$

– *If a complexity reduction is preferred, RHOSVD can be executed by disposing the non-zero singular values and its associated weighting functions, which leads to an approximated model. Also, the transformation is not exact if the rank of any* $\mathfrak{W}_d^{D(\Omega, G)}$*,* $d \in \mathrm{D} \cup \mathrm{H}$ *is smaller than the d-mode rank of* $\mathcal{M}$*.*

- **STEP 3: Reconstruction of the weighting functions**

– *Let* $\mathfrak{W}_n^{D(\omega_n, G_n)} = \mathbf{U}_n$*. All points of the one variable weighting functions* $\mathbf{w}_n(x_n)$ *in equation 1.10 can be constructed from the discretised variants* $\mathfrak{W}_n^{D(\Omega, G)}$ *with any resolution in* ω_n*. E.g. calculating the weighting functions* $\mathbf{w}_d(x_d)$ *along dimension d over a given point* x_d*: through defining a new discretisation grid* G' *as* $G_1 \times \dots \times G_{d-1} \times 1 \times G_{d+1} \times \dots \times G_N$ *and restricting the discretization space to* x_d *as* $\Omega' = \omega_1 \times \dots \times \omega_{d-1} \times x_d \times \omega_{d+1} \times \dots \times \omega_N$*, and defining* $\mathfrak{F}^{D(G', \Omega')}$*,* x_d *results in:*

$$\mathbf{w}_d(x_d) = \mathfrak{F}_{(d)}^{D(G', \Omega')} \left(\mathcal{Q}_{(d)} \right)^+, \tag{1.15}$$

where

$$\mathcal{Q} = \mathcal{S} \underset{\substack{n \in \mathrm{N} \\ n \neq d}}{\boxtimes} \mathfrak{W}_n^{D(\omega_n, G_n)}. \tag{1.16}$$

Here subscript "$()_{(d)}$*" denotes the unfolding along dimension d, accoridng to HOSVD by Lathauwer [34].*

Remark 1 **Transformation error**

A final numerical step can be executed to check the accuracy of the resulting TP model over a large number of random points in the parameter space Ω.

Chapter 2

Statement of the Scientific Student Conference paper

Modern quasi Linear Parameter Varying (qLPV) state-space model and Linear Matrix Inequality (LMI) based multi-objective convex optimization aimed control theories and design methods can be basically divided into three steps:

i) identification of the qLPV state-space model

ii) derivation of the polytopic representation from the qLPV model

iii) substitution of the polytopic representation into LMI based control design methods in order to attain the controller and observer system components

The main focus in the scientific research initiatives was mostly on step *iii*, addressing the investigation and manipulation of LMIs to attain the optimized controller and observer performance, which achieved a significant literature. Moreover, the current widely accepted standpoint among scientific research is represented by the statement that the LMI based control design methods give an optimal solution on the identified qLPV model. However, step *ii*, the effect of the procedure deriving the polytopic model and its effect on the LMI based control design methods was given less attention. A hypothesis published in 2009 [48] discusses and points out this fact that beside the procedure deriving the manipulation of the polytopic representation in step *ii* is necessary and has relatively the same extent of significance as step *iii*, namely the fact that the LMI based control design methods do not give an optimal solution on the identified qLPV model but rather on the polytopic representation at hand and the polytopic manipulation therefore leads to further potential optimization possibilities with a relatively similar importance as the LMI based control design methods.

Goals

In this context the aim of the Scientific Student Conference paper is to systematically investigate and prove the above mentioned - so far unconfirmed - hypothesis both for the control and observer design combined with various polytopic manipulation techniques. As a consequence this proof declares the necessity hence the importance of the polytopic manipulation. In addition a further aim is to show that the manipulation plays an important role in deriving the optimal solution, since the polytopic representation is not invariant. The proof of the hypothesis and the regarding concepts gain further new research directions in the field of qLPV and LMI based control theory research.

Methodology

In order to achieve the above specified goals the paper presents the systematic method which was developed and executed for investigating the hypothesis, its results and consequences which lead to the proof of the hypothesis. The investigation includes the main factors of the polytopic representation influencing the feasibility regions of the LMI based control design, specifically *i)* the manipulation of the vertexes' position and *ii)* the size and complexity of the representation, i.e. the number of the vertexes contained in the TP model type polytopic representation. The proof is based on a complex control design example, where the influence of these factors can be clearly indicated. Furthermore the paper shows via the example that the maximal achievable parameter space of the controller and observer also depend from these factors. The example model consists of the complex Nonlinear Aeroelastic Test Apparatus (NATA) model of the three Degree of Freedom (3-DoF) aeroelastic wing section including Stribeck friction. The methodology is based on the Tensor Product (TP) model transformation based Control Design Framework that supports the flexible manipulation of these factors.

Results and the formulated statement of the Scientific Student Conference paper

Based on the systematical investigation and results the Scientific Student Conference paper presents a TP model transformation based solution to prove the hypothesis via the following statements:

The manipulation of the polytopic TP model representation's Linear Time Invariant (LTI) vertexes influence the feasibility of LMI based control design methods:

i) The position of the LTI vertexes, defining the convex hull of the TP model

type polytopic representation influence the feasibility of LMI based control design.

ii) The complexity of the TP model, namely the number of the LTI vertexes contained in the TP model also influence the feasibility of LMI based control design.

iii) Statement *i)* and *ii)* is valid both for the design of the controller and observer system elements but the influence differs from each other, in fact in certain cases it influences in an opposite way. This may raise further optimization questions: since so far the controller and observer have been designed on the same polytopic representation a design with separate TP model type polytopic representations may induce further benefits.

iv) The position and number of the LTI vertexes of the polytopic TP model representation also influence the size of the achievable parameter space of the feasible design.

Chapter 3

The Methodology for proving the statements

As previously stated the proof in the present paper is based on a control design example of a complex dynamic qLPV system. A TP model representation of the given qLPV system is derived upon which a systematical manipulation and analysis is executed. In accordance to this systematical manipulation LMI based control design theories are applied and the feasibility is checked how it is varying. The manipulation takes the following key points into account:

1) The design is executed both on an exact and on a relaxed TP model representation. The exact representation of the model is derived via the TP model transformation where the number of the vertexes are minimized [39, 40, 41]. The relaxed TP model representation is derived from the exact representation through disposing the vertexes from the model which have low contribution in order to gain a trade-off between accuracy and complexity for further design steps [49]. Note that the relaxed TP model representation is only an approximation of the given model, however its stability verification is performed involving the exact model.

2) The convex hull defined by the position of the vertexes of the TP model representation is systematically modified and analyzed separately for the controller and the observer design.

For each systematically modified case the LMI based control design theory is applied and the feasibility is checked how it is varying. The design method applied in the paper is based on the General TP model transformation based Control Design Framework with the TP model type polytopic formulas [42] and LMI based control design theorems [50, 51].

3.1 The Concepts of the Systematical TP model Manipulation and Investigation

Assume a qLPV state-space model is given as described in 1.1.

$$\begin{pmatrix} \dot{\mathbf{x}}(t) \\ \mathbf{y}(t) \end{pmatrix} = \mathbf{S}(\mathbf{p}(t)) \begin{pmatrix} \mathbf{x}(t) \\ \mathbf{u}(t) \end{pmatrix}.$$

Aim is to control and observe this model. Figure 3.1 shows the system structure with the integrated controller and observer.

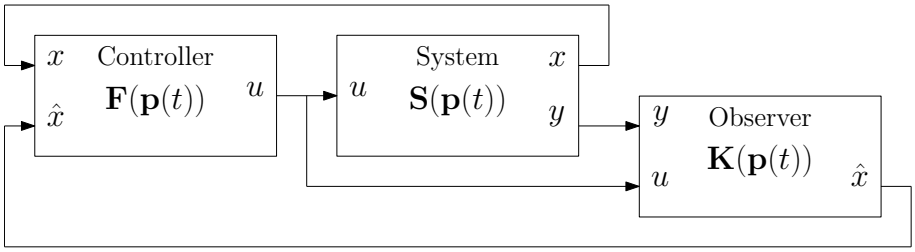

Figure 3.1: *System structure containing the model, controller and observer system components*

Further details of the model and the control design structure will be described in detail later in the present section and in Section 3.1.3. The given model and system components controller and observer take the following TP model structure:

$$\mathbf{S}(\mathbf{p}(t)) = \mathcal{S} \underset{n \in N}{\boxtimes} \mathbf{w}_n(p_n(t)), \tag{3.1}$$

$$\mathbf{F}(\mathbf{p}(t)) = \mathcal{F} \underset{n \in N}{\boxtimes} \mathbf{w}_n(p_n(t)), \tag{3.2}$$

$$\mathbf{K}(\mathbf{p}(t)) = \mathcal{K} \underset{n \in N}{\boxtimes} \mathbf{w}_n(p_n(t)), \tag{3.3}$$

where $\mathbf{S}(\mathbf{p}(t))$ denotes the model, $\mathbf{F}(\mathbf{p}(t))$ denotes the controller and $\mathbf{K}(\mathbf{p}(t))$ denotes the observer.

3.1.1 Step-I: Complexity Relaxation through the main TP model Component Analysis based approach

As a first step of the analysis, the HOSVD based TP model form [39, 40, 41] of the given qLPV model is obtained. Here each singular value represents the relevance of each vertex of the polytopic TP model. By selecting the main TP model components a trade-off between accuracy and complexity is granted in terms of L_2 norm [49]. The complexity relaxation of the model is based on this trade-off: the number of

vertexes contained in the model is decreased through disposing the small singular values and corresponding vertexes which have low contribution.

Thus executing the TP model transformation on $\mathbf{S}(\mathbf{p}(t))$ in Equation 3.1 the following HOSVD based form [39, 40, 41] is acquired:

$$\mathbf{S}(\mathbf{p}(t)) = {}^{\mathcal{E}}\mathcal{S} \underset{n \in N}{\boxtimes} {}^{\mathcal{E}}\mathbf{w}_n(p_n(t)), \tag{3.4}$$

$$\mathcal{S} \in \mathbb{R}^{Q_1 \times \ldots \times Q_N \times O \times I}.$$

Here Q_n is the n-th mode rank of $\mathbf{S}(\mathbf{p}(t))$ c.f. [42] and the superscript "$\mathcal{E}$" denotes that the HOSVD based form of the model is exact, containing all of the non-zero singular values.

On the other hand the relaxed model, represented by the superscript "$\mathcal{R}$", is acquired as well through disposing the singular values and corresponding vertexes with low contribution:

$$\hat{\mathbf{S}}(\mathbf{p}(t)) = {}^{\mathcal{R}}\mathcal{S} \underset{n \in N}{\boxtimes} {}^{\mathcal{R}}\mathbf{w}_n(p_n(t)), \tag{3.5}$$

where ${}^{\mathcal{R}}\mathcal{S} \in \mathbb{R}^{R_1 \times \ldots \times R_n \times O \times I}$ and $\forall n$: $R_n \leq I_n$, $\exists n$: $R_n < I_n$.

3.1.2 Step-II: Convex Hull Manipulation through Interpolation

The LMI design theories applied require a convex TP model representation of the model $\mathbf{S}(\mathbf{p}(t))$ [42, 50]. This being the case the exact and relaxed HOSVD based forms are converted to the convex TP model representation where $\mathbf{S}(\mathbf{p}(t))$ and $\hat{\mathbf{S}}(\mathbf{p}(t))$ are contained and enclosed within their convex hulls defined through the vertexes of their TP models for all $\mathbf{p}(t) \in \Omega$.

The systematical analysis of the convex hulls defined by the position of the vertexes of the TP model representation in the present paper is based on an interpolation technique between two different TP model representations, one with a tight (CNO) and one with a loose (SNNN) convex hull, of the same given qLPV model.

To simplify matters instead of directly interpolating between the two separate convex hulls the interpolation is executed via an interpolation between the two weighting function systems of the two different TP model forms as given in the following: assume two different TP model representations "$\mathcal{X}$" and "$\mathcal{Y}$" of the model

$\mathbf{S}(\mathbf{p}(t))$ are derived through TP model transformation for any parameter $\mathbf{p}(t) \in \Omega$:

$$\begin{aligned} \mathbf{S}(\mathbf{p}(t)) &= {}^{\mathcal{X}}\mathcal{S} \underset{n \in N}{\boxtimes} {}^{\mathcal{X}}\mathbf{w}_n(p_n(t)), \\ \mathbf{S}(\mathbf{p}(t)) &= {}^{\mathcal{Y}}\mathcal{S} \underset{n \in N}{\boxtimes} {}^{\mathcal{Y}}\mathbf{w}_n(p_n(t)). \end{aligned} \tag{3.6}$$

The two different TP model representations "$\mathcal{X}$" and "$\mathcal{Y}$" each possess two different convex hulls specified by the vertexes of the TP model. Aim is to obtain an interpolated TP model representation between these two TP models corresponding to a modifiable interpolation parameter $\lambda \in [0, 1]$:

$$\mathbf{S}(\mathbf{p}(t)) = {}^{\mathcal{I}(\lambda)}\mathcal{S} \underset{n \in N}{\boxtimes} {}^{\mathcal{I}(\lambda)}\mathbf{w}_n(p_n(t)). \tag{3.7}$$

Superscript "$\mathcal{I}(\lambda)$" represents that the TP model representation is interpolated.

Here the weighting function system is interpolated as

$${}^{\mathcal{I}(\lambda)}\mathbf{w}_n(p_n(t)) = (1-\lambda) \cdot {}^{\mathcal{X}}\mathbf{w}_n(p_n(t)) + \lambda \cdot {}^{\mathcal{Y}}\mathbf{w}_n(p_n(t)),$$

and ${}^{\mathcal{I}(\lambda)}\mathcal{S}$ is obtained corresponding to Equation 3.7 by means of the pseudo TP model transformation cf. [45].

Remark 2 Computational aspects of the interpolation: *The TP model transformation generates the discretized variants* ${}^{\mathcal{X}}\mathfrak{W}_n^{D(\Omega,G)}$ *and* ${}^{\mathcal{Y}}\mathfrak{W}_n^{D(\Omega,G)}$ *(see Equation 3.18) on the parameter space* Ω *with grid* $G_1 \times \cdots \times G_N$ *of the weighting functions* ${}^{\mathcal{X}}\mathbf{w}_n(p_n(t))$ *and* ${}^{\mathcal{Y}}\mathbf{w}_n(p_n(t))$ *(see Equation 3.6), respectively. The discretized variants of the weighting functions* $\mathfrak{W}_n^{D(\Omega,G)}$ *are also the n-mode singular matrices* $\mathfrak{W}_n^{D(\Omega,G)} = U_n$*. Thus the interpolation is simplified and the interpolated discretized weighting functions take the following form:*

$${}^{\mathcal{I}(\lambda)}\mathfrak{W}_n^{D(\Omega,G)} = (1-\lambda) \cdot {}^{\mathcal{X}}\mathfrak{W}_n^{D(\Omega,G)} + \lambda \cdot {}^{\mathcal{Y}}\mathfrak{W}_n^{D(\Omega,G)}.$$

In the case if ${}^{\mathcal{I}(\lambda)}\mathfrak{W}_n^{D(\Omega,G)}$ *and* $\mathbf{S}(\mathbf{p}(t))$ *are available* ${}^{\mathcal{I}(\lambda)}\mathcal{S}$ *and* ${}^{\mathcal{I}(\lambda)}\mathbf{w}_n(p_n(t))$ *for Equation 3.7 can be similarly determined with the help of the pseudo TP model transformation as mentioned in Section 3.1.2.*

3.1.3 Step-III: LMI Based Design Theorems

As previously described in Section 3.1 the aim is to control and observe the given qLPV model. Since in the model only a part of the state variables are measurable an output feedback based control design structure is applied and the rest of the state variables are approximated by an observer. Because the parameter vector $\mathbf{p}(t)$ does

not include elements from the estimated state-vector $\hat{\mathbf{x}}(t)$, the following controller and observer structure is applied [51, 50, 42]:

$$\begin{aligned}\dot{\hat{\mathbf{x}}}(t) &= \mathbf{A}(\mathbf{p}(t))\hat{\mathbf{x}}(t) + \mathbf{B}(\mathbf{p}(t))\mathbf{u}(t) + \mathbf{K}(\mathbf{p}(t))(\mathbf{y}(t) - \hat{\mathbf{y}}(t)) \\ \hat{\mathbf{y}}(t) &= \mathbf{C}(\mathbf{p}(t))\hat{\mathbf{x}}(t) \\ \mathbf{u}(t) &= -\mathbf{F}(\mathbf{p}(t))\mathbf{x}(t),\end{aligned} \tag{3.8}$$

otherwise written as:

$$\begin{aligned}\begin{pmatrix}\dot{\hat{\mathbf{x}}}(t) \\ \hat{\mathbf{y}}(t)\end{pmatrix} &= \mathbf{S}(\mathbf{p}(t)) \begin{pmatrix}\hat{\mathbf{x}}(t) \\ \mathbf{u}(t)\end{pmatrix} + \begin{pmatrix}\mathbf{K}(\mathbf{p}(t)) \\ 0\end{pmatrix} (\mathbf{y}(t) - \hat{\mathbf{y}}(t)) \\ \mathbf{u}(t) &= -\mathbf{F}(\mathbf{p}(t))\mathbf{x}(t).\end{aligned} \tag{3.9}$$

The observer is required to satisfy the convergence for stability $\mathbf{x}(t) - \hat{\mathbf{x}}(t) \to 0 \quad \text{as} \quad t \to \infty$.

As previously mentioned one of the main benefits of the General TP model transformation based Control Design Framework is that the controller and observer system components can be acquired separately. This ensures that the convex hull analysis can be performed also separately for the controller and the observer.

The aim through the LMI based design is to acquire controller vertex gains $\mathbf{F}_{i_1,\, i_2,\, ...,\, i_N}$ stored in $\mathcal{F}$ from vertex gains $\mathbf{S}_{i_1,\, i_2,\, ...,\, i_N}$ stored in ${}^{\mathcal{I}(\lambda_c)}\mathcal{S}$

$$\mathbf{S}(\mathbf{p}(t)) = {}^{\mathcal{I}(\lambda_c)}\mathcal{S} \underset{n \in N}{\boxtimes} {}^{\mathcal{I}(\lambda_c)}\mathbf{w}_n(p_n(t))$$

and observer vertex gains $\mathbf{K}_{i_1,\, i_2,\, ...,\, i_N}$ stored in $\mathcal{K}$ from $\mathbf{S}_{i_1,\, i_2,\, ...,\, i_N}$ stored in ${}^{\mathcal{I}(\lambda_o)}\mathcal{S}$

$$\mathbf{S}(\mathbf{p}(t)) = {}^{\mathcal{I}(\lambda_o)}\mathcal{S} \underset{n \in N}{\boxtimes} {}^{\mathcal{I}(\lambda_o)}\mathbf{w}_n(p_n(t)),$$

in a way that the stability and the desired multi-objective control performance requirements are guaranteed. The superscripts "$\mathcal{I}(\lambda_c)$" and "$\mathcal{I}(\lambda_o)$" represent the proportion along the interpolation for both controller and observer cases, respectively.

Various LMI theorems are accessible for controller and observer design. For the separate design the following LMI theorems have been chosen [50].

Theorem 1 Globally and asymptotically stable controller: *Assume the polytopic model (3.1) with a controller of structure (3.2) is given. This output-feedback control structure is globally and asymptotically stable if the matrices* $\mathbf{P}_1 > \mathbf{0}$ *and* $\mathbf{M}_r$ *exist,* ($r = 1, \ldots, R$ *where* R *denotes the number of LTI vertex systems) satisfying*

equations:

$$\begin{aligned}
&\mathbf{P}_1\mathbf{A}_r^T - \mathbf{M}_r^T\mathbf{B}_r^T + \mathbf{A}_r\mathbf{P}_1 - \mathbf{B}_r\mathbf{M}_r \qquad &< \mathbf{0},\\
&\\
&\mathbf{P}_1\mathbf{A}_r^T - \mathbf{M}_s^T\mathbf{B}_r^T + \mathbf{A}_s\mathbf{P}_1 - \mathbf{B}_r\mathbf{M}_s + \\
&\mathbf{P}_1\mathbf{A}_s^T - \mathbf{M}_r^T\mathbf{B}_s^T + \mathbf{A}_s\mathbf{P}_1 - \mathbf{B}_s\mathbf{M}_r \qquad &< \mathbf{0}
\end{aligned}$$

for $r < s \leq R$, except the pairs (r, s) such that $\forall \mathbf{p}(t) : w_r(\mathbf{p}(t))w_s(\mathbf{p}(t)) = 0$, and where $\mathbf{M}_r = \mathbf{F}_r\mathbf{P}_1$. The controller feedback gains can then be obtained from the solution of the above LMIs as $\mathbf{F}_r = \mathbf{M}_r\mathbf{P}_1^{-1}$.

Theorem 2 Globally and asymptotically stable observer: *Assume the polytopic model (3.1) with an observer of structure (3.3) is given. This observer structure is globally and asymptotically stable if the matrices $\mathbf{P}_2 > \mathbf{0}$ and $\mathbf{N}_r$ exist, ($r = 1$, $\ldots$, R where R denotes the number of LTI vertex systems) satisfying equations:*

$$\begin{aligned}
&\mathbf{A}_r^T\mathbf{P}_2 - \mathbf{C}_r^T\mathbf{N}_r^T + \mathbf{P}_2\mathbf{A}_r - \mathbf{N}_r\mathbf{C}_r \qquad &< \mathbf{0},\\
&\\
&\mathbf{A}_r^T\mathbf{P}_2 - \mathbf{C}_s^T\mathbf{N}_r^T + \mathbf{P}_2\mathbf{A}_r - \mathbf{N}_r\mathbf{C}_s + \\
&\mathbf{A}_s^T\mathbf{P}_2 - \mathbf{C}_r^T\mathbf{N}_s^T + \mathbf{P}_2\mathbf{A}_s - \mathbf{N}_s\mathbf{C}_r \qquad &< \mathbf{0}
\end{aligned}$$

for $r < s \leq R$, except the pairs (r, s) such that $\forall \mathbf{p}(t) : w_r(\mathbf{p}(t))w_s(\mathbf{p}(t)) = 0$, and where $\mathbf{N}_r = \mathbf{P}_2\mathbf{K}_r$. The observer gains can then be obtained from the solution of the above LMIs as $\mathbf{K}_r = \mathbf{P}_2^{-1}\mathbf{N}_r$.

Computing the controller and observers via the LMI based design Theorems 1 and 2 one attains the results:

$$^{\lambda_c}\mathbf{F}(\mathbf{p}(t)) = {}^{\lambda_c}\mathcal{F} \underset{n\in N}{\boxtimes}{}^{\mathcal{I}(\lambda_c)}\mathbf{w}_n(p_n(t)), \tag{3.10}$$

$$^{\lambda_o}\mathbf{K}(\mathbf{p}(t)) = {}^{\lambda_o}\mathcal{K} \underset{n\in N}{\boxtimes}{}^{\mathcal{I}(\lambda_o)}\mathbf{w}_n(p_n(t)). \tag{3.11}$$

It is worth mentioning that various further control objectives and constraints can be incorporated to the design via properly selected LMIs as well.

3.1.4 Step-IV: Exact System Reconstruction

To verify the stability of the system LMI based stability verification theorems can be executed with the system elements (3.1-3.3). Here a uniform structure is required from the system components to be able to execute the stability verification theorems

for the system. However the uniform structure is not provided, due to the systematical complexity (Section 3.1.1) and convex hull (Section 3.1.2) manipulation the system components have different weighting functions varying in number and form:

$$\mathbf{S}(\mathbf{p}(t)) = {}^{\mathcal{E}}\mathcal{S} \underset{n\in N}{\boxtimes} {}^{\mathcal{E}}\mathbf{w}_n(p_n(t)), \tag{3.12}$$

$${}^{\lambda_c}\mathbf{F}(\mathbf{p}(t)) = {}^{\lambda_c}\mathcal{F} \underset{n\in N}{\boxtimes} {}^{\mathcal{F}}\mathbf{w}_n(p_n(t)), \tag{3.13}$$

$${}^{\lambda_o}\mathbf{K}(\mathbf{p}(t)) = {}^{\lambda_o}\mathcal{K} \underset{n\in N}{\boxtimes} {}^{\mathcal{K}}\mathbf{w}_n(p_n(t)). \tag{3.14}$$

Here ${}^{\mathcal{F}}\mathbf{w}_n(p_n(t)) = {}^{\mathcal{I}(\lambda_c)}\mathbf{w}_n(p_n(t))$ and ${}^{\mathcal{K}}\mathbf{w}_n(p_n(t)) = {}^{\mathcal{I}(\lambda_o)}\mathbf{w}_n(p_n(t))$. As a consequence an additional step is required to unify the structure of the system elements to be able to execute the LMI based stability verification theorems.

It is important to mention that the exact model represented by superscript "$\mathcal{E}$" is used for the stability verification. This means that the manipulated and analyzed controller and observer vertexes may differ from the exact model in their number along some dimensions. In this context in order to apply the LMI based stability verification techniques a common weighting function system has to be attained. One way to do this is to apply the general stability verification method based on the Multi TP model transformation [45]. However because during the calculations the discrete variants of the interpolated weighting functions will be available a less complicated procedure can be applied to unify the weighting functions.

Thus in this context the aim is to convert Equations 3.12-3.14 to 3.15-3.17:

$$\mathbf{S}(\mathbf{p}(t)) = {}^{\mathcal{E}}\mathcal{S}' \underset{n\in N}{\boxtimes} \mathbf{w}_n(p_n(t)), \tag{3.15}$$

$${}^{\lambda_c}\mathbf{F}(\mathbf{p}(t)) = {}^{\lambda_c}\mathcal{F}' \underset{n\in N}{\boxtimes} \mathbf{w}_n(p_n(t)), \tag{3.16}$$

$${}^{\lambda_o}\mathbf{K}(\mathbf{p}(t)) = {}^{\lambda_o}\mathcal{K}' \underset{n\in N}{\boxtimes} \mathbf{w}_n(p_n(t)). \tag{3.17}$$

As a first step a matrix $\mathbf{H}_n$ for each dimension is created as:

$$\mathbf{H}_n = [{}^{\mathcal{I}(\lambda_c)}\mathfrak{W}_{\mathbf{n}}^{D(\Omega,G)}, {}^{\mathcal{I}(\lambda_o)}\mathfrak{W}_{\mathbf{n}}^{D(\Omega,G)}, {}^{\mathcal{E}}\mathfrak{W}_{\mathbf{n}}^{D(\Omega,G)}], \tag{3.18}$$

where $\mathfrak{W}_n^{D(\Omega,G)}$ are the discretized variants of the weighting functions of the TP model over the parameter space Ω with sampling grid G [45]. Executing a compact SVD on matrix $\mathbf{H}_n$ one attains:

$$\mathbf{H}_n = \mathbf{U}_n\mathbf{D}_n\mathbf{V}_n^T = \mathbf{U}_n\mathbf{T}_n.$$

Since system elements (3.12-3.14) require a convex representation, the SVD is ex-

tended with a CNO transformation [42]. This leads to:

$$\mathbf{H}_n = \mathbf{U}_n^{\mathcal{CNO}} \mathbf{T'}_n,$$

where $\mathbf{U}_n^{\mathcal{CNO}}$ is the discretized variant of the unified weighting function.

$$\mathfrak{W}_n^{D(\Omega,G)} = \mathbf{U}_n^{\mathcal{CNO}}.$$

Partitioning the matrix $\mathbf{T'}_n$ according to the extent of the blocks of $\mathbf{H}_n$ (Equation 3.18), one acquires:

$$\mathbf{T'}_n = [{}^{\mathcal{F}}\mathbf{T}_n, {}^{\mathcal{K}}\mathbf{T}_n, {}^{\mathcal{E}}\mathbf{T}_n],$$

which results in

$$\begin{aligned}
{}^{\mathcal{I}(\lambda_c)}\mathfrak{W}_n^{D(\Omega,G)} &= \mathbf{U}_n^{\mathcal{CNO}} \cdot {}^{\mathcal{F}}\mathbf{T}_n, \\
{}^{\mathcal{I}(\lambda_o)}\mathfrak{W}_n^{D(\Omega,G)} &= \mathbf{U}_n^{\mathcal{CNO}} \cdot {}^{\mathcal{K}}\mathbf{T}_n, \\
{}^{\mathcal{E}}\mathfrak{W}_n^{D(\Omega,G)} &= \mathbf{U}_n^{\mathcal{CNO}} \cdot {}^{\mathcal{E}}\mathbf{T}_n,
\end{aligned}$$

and

$$\begin{aligned}
\mathbf{S}(\mathbf{p}(t)) &= {}^{\mathcal{E}}\mathcal{S} \boxtimes_{n\in N} {}^{\mathcal{E}}\mathfrak{W}_n^{D(\Omega,G)} = \\
&= {}^{\mathcal{E}}\mathcal{S} \boxtimes_{n\in N} \mathbf{U}_n^{\mathcal{CNO}} \cdot {}^{\mathcal{E}}\mathbf{T}_n = \\
&= [{}^{\mathcal{E}}\mathcal{S} \boxtimes_{n\in N} {}^{\mathcal{E}}\mathbf{T}_n] \boxtimes_{n\in N} \mathbf{U}_n^{\mathcal{CNO}} = \\
&= {}^{\mathcal{E}}\mathcal{S}' \boxtimes_{n\in N} \mathbf{U}_n^{\mathcal{CNO}} = \\
&= {}^{\mathcal{E}}\mathcal{S}' \boxtimes_{n\in N} \mathfrak{W}_n^{D(\Omega,G)},
\end{aligned}$$

$$\begin{aligned}
\mathbf{F}(\mathbf{p}(t)) &= {}^{\mathcal{E}}\mathcal{F} \boxtimes_{n\in N} {}^{\mathcal{E}}\mathfrak{W}_n^{D(\Omega,G)} = \\
&= {}^{\mathcal{E}}\mathcal{F} \boxtimes_{n\in N} \mathbf{U}_n^{\mathcal{CNO}} \cdot {}^{\mathcal{E}}\mathbf{T}_n = \\
&= [{}^{\mathcal{E}}\mathcal{F} \boxtimes_{n\in N} {}^{\mathcal{E}}\mathbf{T}_n] \boxtimes_{n\in N} \mathbf{U}_n^{\mathcal{CNO}} = \\
&= {}^{\mathcal{E}}\mathcal{F}' \boxtimes_{n\in N} \mathbf{U}_n^{\mathcal{CNO}} = \\
&= {}^{\mathcal{E}}\mathcal{F}' \boxtimes_{n\in N} \mathfrak{W}_n^{D(\Omega,G)},
\end{aligned}$$

$$
\begin{aligned}
\mathbf{K}(\mathbf{p}(t)) &= {}^{\mathcal{E}}\mathcal{K} \underset{n\in N}{\boxtimes} {}^{\mathcal{E}}\mathfrak{W}_n^{D(\Omega,G)} = \\
&= {}^{\mathcal{E}}\mathcal{K} \underset{n\in N}{\boxtimes} \mathbf{U}_n^{\mathcal{CNO}} \cdot {}^{\mathcal{E}}\mathbf{T}_n = \\
&= [{}^{\mathcal{E}}\mathcal{K} \underset{n\in N}{\boxtimes} {}^{\mathcal{E}}\mathbf{T}_n] \underset{n\in N}{\boxtimes} \mathbf{U}_n^{\mathcal{CNO}} = \\
&= {}^{\mathcal{E}}\mathcal{K}' \underset{n\in N}{\boxtimes} \mathbf{U}_n^{\mathcal{CNO}} = \\
&= {}^{\mathcal{E}}\mathcal{K}' \underset{n\in N}{\boxtimes} \mathfrak{W}_n^{D(\Omega,G)}.
\end{aligned}
$$

Finally, the continuous weighting functions $\mathbf{w}_n(p_n(t))$ can also be obtained through the Pseudo TP model transformation [45] as described in Step-II in Section 3.1.2.

3.1.5 Step-V: LMI based stability verification

Acquiring the system components ${}^{\mathcal{E}}\mathcal{S}'$, ${}^{\mathcal{F}}\mathcal{S}'$ and ${}^{\mathcal{K}}\mathcal{S}'$ with unified weighting function systems $\mathfrak{W}_n^{D(\Omega,G)}$ the LMI based stability verification can be readily applied. The vertices of the TP model of the exact model, controller and observer can be substituted into the previously described LMI theorems in Section 3.1.3 and the solution can be checked, namely if all of the LMI theorems are simultaneously feasible. This step is less complicated in a sense that the matrices N and M need not to be found, only the matrices P_1 and P_2 need to be found.

3.2 The Example Model

In this section the state-space qLPV model of the three Degree of Freedom (3-DoF) aeroelastic wing section model including Stribeck friction of the complex Nonlinear Aeroelastic Test Apparatus (NATA) model [52, 53, 54] will be described. Active control of aeroelasticity has been a major topic of discussion in aerospace and control engineering for several years. Several studies can be found discussing the analysis and different control design strategies of the aeroelastic wing section [55, 56, 57, 58, 59, 60, 61, 62, 63, 54, 64, 65, 66, 67, 68, 69, 70, 71, 72, 73, 74, 75, 76]. The aeroelastic wing section model is an effective example for discussing the analysis and different control design strategies of aeroelasticity. The TP model transformation based control solutions to the 2-DoF and the 3-DoF aeroelastic wing section are given in [62, 63, 77, 52].

The state-space qLPV model of the 3-DoF aeroelastic wing section including

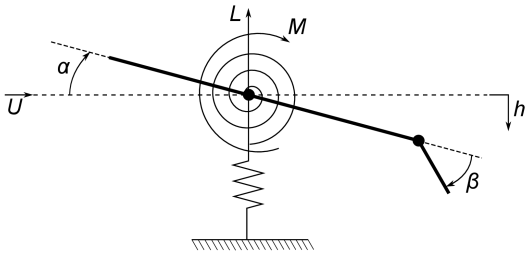

Figure 3.2: *3-DoF aeroelastic wing section and state variables [42]*

friction [52] is given similarly to Equation 1.1:

$$\begin{pmatrix} \dot{\mathbf{x}}(t) \\ \mathbf{y}(t) \end{pmatrix} = \mathbf{S}(\mathbf{p}(t)) \begin{pmatrix} \mathbf{x}(t) \\ \mathbf{u}(t) \end{pmatrix}.$$

The state vector consists of

$$\begin{aligned} \mathbf{x}(t) &= \begin{pmatrix} \mathbf{x}_1(t) & \mathbf{x}_2(t) & \mathbf{x}_3(t) & \mathbf{x}_4(t) & \mathbf{x}_5(t) & \mathbf{x}_6(t) \end{pmatrix}^T \\ &= \begin{pmatrix} \dot{h} & \dot{\alpha} & \dot{\beta} & h & \alpha & \beta \end{pmatrix}^T, \end{aligned}$$

where h symbolizes the plunge, α symbolizes the pitch and β symbolizes the trailing-edge surface deflection of the aeroelastic wing section. The elements can be seen in Figure 3.2. The time varying parameter vector consists of $\mathbf{p}(t) = \begin{pmatrix} U(t) & \alpha(t) & \dot{\beta}(t) \end{pmatrix}^T \in \Omega$. $U(t)$ represents the wind speed, $\alpha(t)$ represents the above mentioned pitch and $\dot{\beta}(t)$ is introduced by the friction model. As the parameter vector $\mathbf{p}(t)$ contains elements of the state vector $\mathbf{x}(t)$, the state-space model belongs to the class of qLPV state-space systems. The elements of $\mathbf{S}(\mathbf{p}(t))$ are:

$$\begin{aligned} \mathbf{A}(\mathbf{p}(t)) &= \begin{pmatrix} -\mathbf{M}^{-1}\mathbf{C}(\mathbf{p}(t)) & -\mathbf{M}^{-1}\mathbf{K}(\mathbf{p}(t)) \\ -\mathbf{I} & 0 \end{pmatrix}, \\ \mathbf{B} &= \begin{pmatrix} \mathbf{M}^{-1}\mathbf{F} \\ 0 \end{pmatrix}, \\ \mathbf{C} &= \begin{pmatrix} 0 & 0 & 0 & 0 & 1 & 0 \end{pmatrix}, \\ \mathbf{D} &= 0, \end{aligned} \tag{3.19}$$

where the matrices $\mathbf{M}$, $\mathbf{C}$, $\mathbf{K}$ and $\mathbf{F}$ are the mass, damping, stiffness and forcing matrices of the equation of motion:

$$\mathbf{M}\begin{pmatrix}\ddot{h}\\ \ddot{\alpha}\\ \ddot{\beta}\end{pmatrix}+\mathbf{C}\begin{pmatrix}\dot{h}\\ \dot{\alpha}\\ \dot{\beta}\end{pmatrix}+\mathbf{K}\begin{pmatrix}h\\ \alpha\\ \beta\end{pmatrix}=\mathbf{Fu}. \tag{3.20}$$

These matrices take the following form:

$$\mathbf{M}=\begin{pmatrix} m_h+m_\alpha+m_\beta & m_a x_a b+m_\beta r_\beta+m_\beta x_\beta & m_\beta r_\beta \\ m_a x_a b+m_\beta r_\beta+m_\beta x_\beta & \hat{I}_\alpha+\hat{I}_\beta+m_\beta r_\beta^2+2x_\beta m_\beta r_\beta & \hat{I}_\beta+x_\beta m_\beta r_\beta \\ m_\beta r_\beta & \hat{I}_\beta+x_\beta m_\beta r_\beta & \hat{I}_\beta \end{pmatrix},$$

$$\mathbf{C}=\begin{pmatrix} c_h+\rho b S C_{l_\alpha} U & \left(\frac{1}{2}-a\right) b\rho b S C_{l_\alpha} U & 0 \\ -\rho b^2 S C_{m_{\alpha,eff}} U & c_\alpha-\left(\frac{1}{2}-a\right) b\rho b^2 S C_{m_{\alpha,eff}} U & 0 \\ 0 & 0 & c_{\beta_{servo}} \end{pmatrix},$$

$$\mathbf{K}=\begin{pmatrix} k_h & \rho b S C_{l_\alpha} U^2 & \rho b S C_{l_\beta} U^2 \\ 0 & k_\alpha(\alpha)-\rho b^2 S C_{m_{\alpha,eff}} U^2 & -\rho b^2 S C_{m_{\beta,eff}} U^2 \\ 0 & 0 & k_{\beta_{servo}} \end{pmatrix},$$

$$\mathbf{F}=\begin{pmatrix} 0 \\ 0 \\ k_{\beta_{servo}} \end{pmatrix}.$$

The model is attained from the equation of motion through the following, substituting the matrices $\mathbf{M}$, $\mathbf{C}$, $\mathbf{K}$ and $\mathbf{F}$ into the equation of motion:

$$\begin{pmatrix} m_h+m_\alpha+m_\beta & m_a x_a b+m_\beta r_\beta+m_\beta x_\beta & m_\beta r_\beta \\ m_a x_a b+m_\beta r_\beta+m_\beta x_\beta & \hat{I}_\alpha+\hat{I}_\beta+m_\beta r_\beta^2+2x_\beta m_\beta r_\beta & \hat{I}_\beta+x_\beta m_\beta r_\beta \\ m_\beta r_\beta & \hat{I}_\beta+x_\beta m_\beta r_\beta & \hat{I}_\beta \end{pmatrix}\begin{pmatrix}\ddot{h}\\ \ddot{\alpha}\\ \ddot{\beta}\end{pmatrix}+$$
$$+\begin{pmatrix} c_h & 0 & 0 \\ 0 & c_\alpha & 0 \\ 0 & 0 & c_{\beta_{servo}} \end{pmatrix}\begin{pmatrix}\dot{h}\\ \dot{\alpha}\\ \dot{\beta}\end{pmatrix}+\begin{pmatrix} k_h & 0 & 0 \\ 0 & k_\alpha(\alpha) & 0 \\ 0 & 0 & k_{\beta_{servo}} \end{pmatrix}\begin{pmatrix}h\\ \alpha\\ \beta\end{pmatrix}=\begin{pmatrix} -L \\ M \\ k_{\beta_{servo}}\beta_{des} \end{pmatrix},$$

where $k_\alpha(\alpha)$ is obtained in [54] by curve fitting on the measured displacement-moment data for a nonlinear spring $k_\alpha(\alpha) = 25.55 - 103.19\alpha + 543.24\alpha^2$. It is important to emphasize that the order of the polynomial defining $k_\alpha(\alpha)$ does not influence the control design methodology. Hence, one can apply a higher order polynomial to model the non linearity of the spring, which can be found in [58] dealing with the aeroelastic wing section model .

Quasi-steady aerodynamic force L and moment M are assumed in the same way found in the sources in their control design approaches:

$$L=\rho U^2 b C_{l_\alpha}\left(\alpha+\frac{\dot{h}}{U}+\left(\frac{1}{2}-a\right)b\frac{\dot{\alpha}}{U}\right)+\rho U^2 b c_{l_\beta}\beta \tag{3.21}$$

$$M = \rho U^2 b^2 C_{m_{\alpha,eff.}} \left(\alpha + \frac{\dot{h}}{U} + \left(\frac{1}{2} - a \right) b \frac{\dot{\alpha}}{U} \right) + \rho U^2 b C_{m_{\beta,eff.}} \beta \tag{3.22}$$

The above L and M above are accurate for the low-velocity regime.

Based on [54], it is assumed that the trailing-edge servo-motor dynamics can be represented using a second-order system of the form:

$$\hat{I}_\beta \ddot{\beta} + c_{\beta_{servo}} \dot{\beta} + k_{\beta_{servo}} \beta = k_{\beta_{servo}} \mathbf{u}_\beta. \tag{3.23}$$

By combining equations 3.20, 3.21, 3.22 and 3.23 one obtains:

$$\underbrace{\begin{pmatrix} m_h + m_\alpha + m_\beta & m_a x_a b + m_\beta r_\beta + m_\beta x_\beta & m_\beta r_\beta \\ m_a x_a b + m_\beta r_\beta + m_\beta x_\beta & \hat{I}_\alpha + \hat{I}_\beta + m_\beta r_\beta^2 + 2 x_\beta m_\beta r_\beta & \hat{I}_\beta + x_\beta m_\beta r_\beta \\ m_\beta r_\beta & \hat{I}_\beta + x_\beta m_\beta r_\beta \hat{I}_\beta m x_\alpha b & I_\alpha \end{pmatrix}}_{\mathbf{M}} \begin{pmatrix} \ddot{h} \\ \ddot{\alpha} \\ \ddot{\beta} \end{pmatrix} +$$

$$+ \underbrace{\begin{pmatrix} c_h + \rho b S C_{l_\alpha} U & \left(\frac{1}{2} - a\right) b \rho b S C_{l_\alpha} U & 0 \\ -\rho b^2 S C_{m_{\alpha,eff}} U & c_\alpha - \left(\frac{1}{2} - a\right) b \rho b^2 S C_{m_{\alpha,eff}} U & 0 \\ 0 & 0 & c_{\beta_{servo}} \end{pmatrix}}_{\mathbf{C}} \begin{pmatrix} \dot{h} \\ \dot{\alpha} \\ \dot{\beta} \end{pmatrix} +$$

$$+ \underbrace{\begin{pmatrix} k_h & \rho b S C_{l_\alpha} U^2 & \rho b S C_{l_\beta} U^2 \\ 0 & k_\alpha(\alpha) - \rho b^2 S C_{m_{\alpha,eff}} U^2 & -\rho b^2 S C_{m_{\beta,eff}} U^2 \\ 0 & 0 & k_{\beta_{servo}} \end{pmatrix}}_{\mathbf{K}} \begin{pmatrix} h \\ \alpha \\ \beta \end{pmatrix} = \underbrace{\begin{pmatrix} 0 \\ 0 \\ k_{\beta_{servo}} \end{pmatrix}}_{\mathbf{F}} \mathbf{u}.$$

where **M**, **C**, **K** and **F** are the previously mentioned mass, damping, stiffness and forcing matrices of the equation of motion [54] in Equation 3.20.

The details and definition of each system parameter can be found in [54] and they have the following values: $m_h = 6.516\ kg$; $m_\alpha = 6.7\ kg$; $m_\beta = 0.537\ kg$; $x_\alpha = 0.21$; $x_\beta = 0.233$; $r_\beta = 0\ m$; $a = -0.673\ m$; $b = 0.1905\ m$; $\hat{I}_\alpha = 0.126\ kgm^2$; $\hat{I}_\beta = 10^{-5}$; $c_h = 27.43\ Nms/rad$; $c_\alpha = 0.215\ Nms/rad$; $c_{\beta_{servo}} = 4.182 * 10^{-4}\ Nms/rad$; $k_h = 2844$; $k_{\beta_{servo}} = 7.6608 * 10^{-3}$; $\rho = 1.225\ kg/m^3$; $C_{l_\alpha} = 6.757$; $C_{m_{\alpha,eff}} = -1.17$; $C_{l_\beta} = 3.774$; $C_{m_{\beta,eff}} = -2.1$; $S = 0.5945\ m$.

The system matrix $\mathbf{S}(\mathbf{p}(t))$ of the given qLPV model includes the Stribeck friction model defined in the following where $F_f(t)$ represents the friction force:

$$F_f(t) = - \left(F_c + \frac{(F_s - F_c)}{\left(1 + \left(\frac{v}{v_s}\right)^2\right)} \right) \text{sign}(v(t)) - F_v v,$$

where $sign(v(t)) = \frac{2}{1+e^{-1000 \cdot v(t)}} - 1$ and $v(t) \neq 0$. The parameter v_s represents the Stribeck velocity, F_s represents the static friction force, F_c represents the Coulomb friction force and F_v represents the viscous friction force. The values of these elements were defined based on engineering considerations in order to obtain a realistic friction model. The values are $F_v = F_c = 4.182 \cdot 10^{-4}\ Nm$ for the viscous friction and Coulomb friction force term, $F_s = 1.2 \cdot F_c$ for the Stribeck friction force term and $v_s = 0.0075\ rad/s$ for the Stribeck velocity. Further details and definitions of the parameters can be found in [54, 52]. It is important to mention that the control design and assessments in this paper is a general method, hence other nonlinear friction models can also be applied.

Chapter 4

The Results for proving the statement

In this section the previously described theoretical analysis concepts will be applied into practice on the example model of the 3-DoF wing section accompanied by presenting the proving results.

4.1 Numerical execution of the Tensor Product model transformation based Control Design Framework

The TP model transformation is performed on the state-space qLPV model of the 3-DoF aeroelastic wing section model described in Section 3.2. The parameter vector $\mathbf{p}(t)$ is specified through the intervals of the elements $U \in [4,\ 64]$ (m/s) (later this interval will be systematically modified and investigated), $\alpha \in [-0.3,\ 0.3]$ (rad) and $\dot{\beta} \in [-1.5, 1.5]$ (rad/s). The grid density $G_1 \times G_2 \times G_3$ is specified as $G_1 = G_2 = 501$ and $G_3 = 7500$. The rank of the discretized core tensor $\mathcal{S}^{D(\Omega,G)}$ results in 2, 3, 2 in the first, second and third dimensions, therefore $2 \times 3 \times 2 = 12$ vertexes describe the exact polytopic TP model representation of the given qLPV state-space model. To acquire the relaxed polytopic TP model representation of the given qLPV state-space model the third singular value 0.02275 in dimension $\alpha(t)$ is disposed. The singular values along each dimension take the following values:

Dimension $U(t)$:	1824.42567	222.73378	
Dimension $\alpha(t)$:	1837.72468	30.12274	0.02275
Dimension $\dot{\beta}(t)$:	1478.89237	1091.33713	

To systematically modify and analyze the convex hull defined by the position of the vertexes of the TP model representation through interpolation two types of TP model representations are determined: one with a loose (SNNN: $\lambda = 0\%$) and one

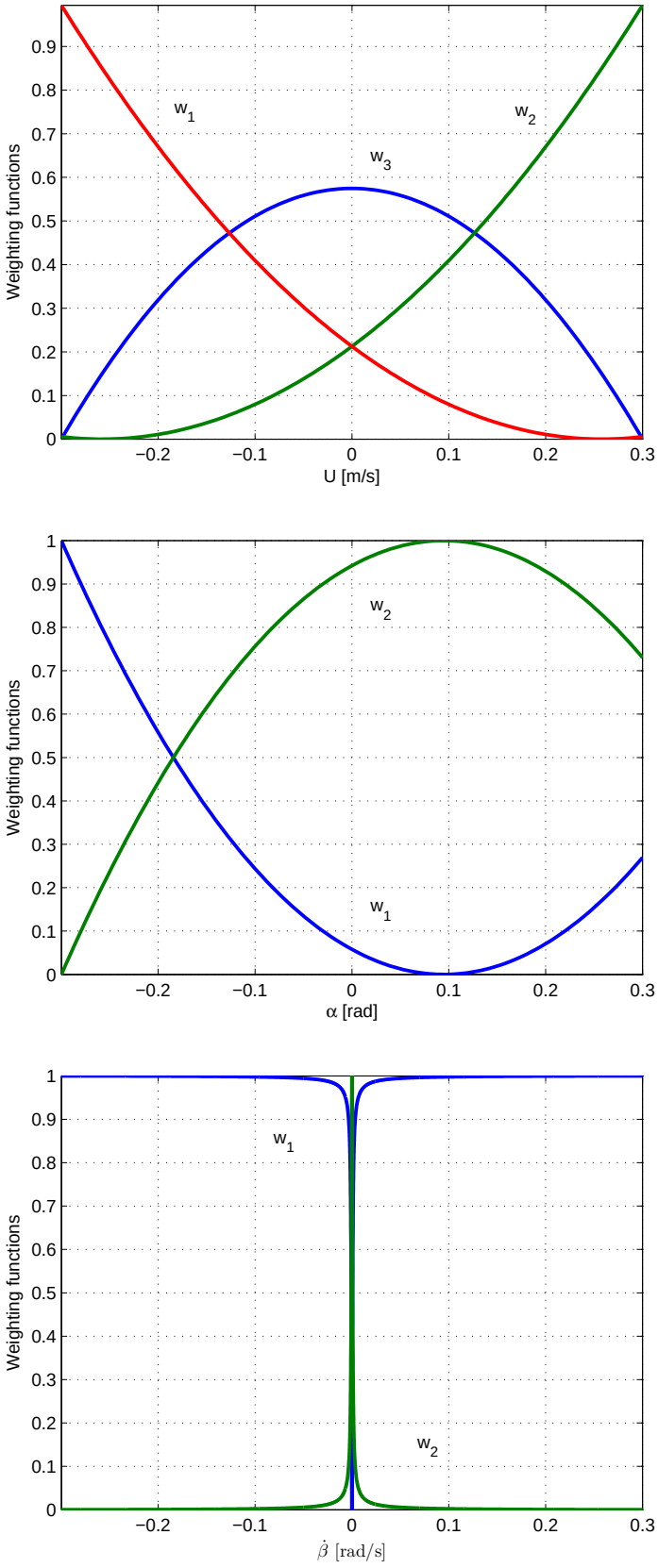

Figure 4.1: *CNO type weighting functions of the exact model for each dimension* $U[m/s]$, $\alpha[rad]$, $\dot{\beta}[rad/s]$

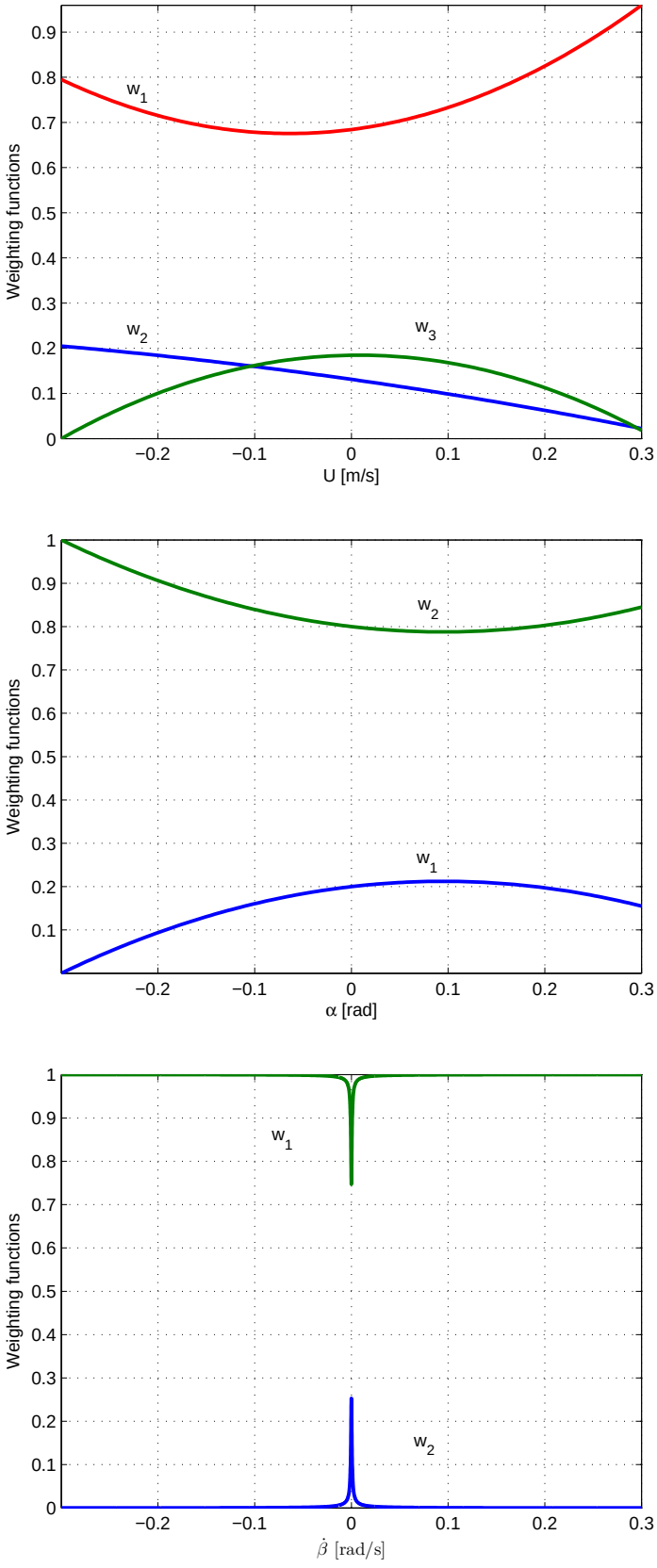

Figure 4.2: *SNNN type weighting functions of the exact model for each dimension* $U[m/s]$, $\alpha[rad]$, $\dot{\beta}[rad/s]$

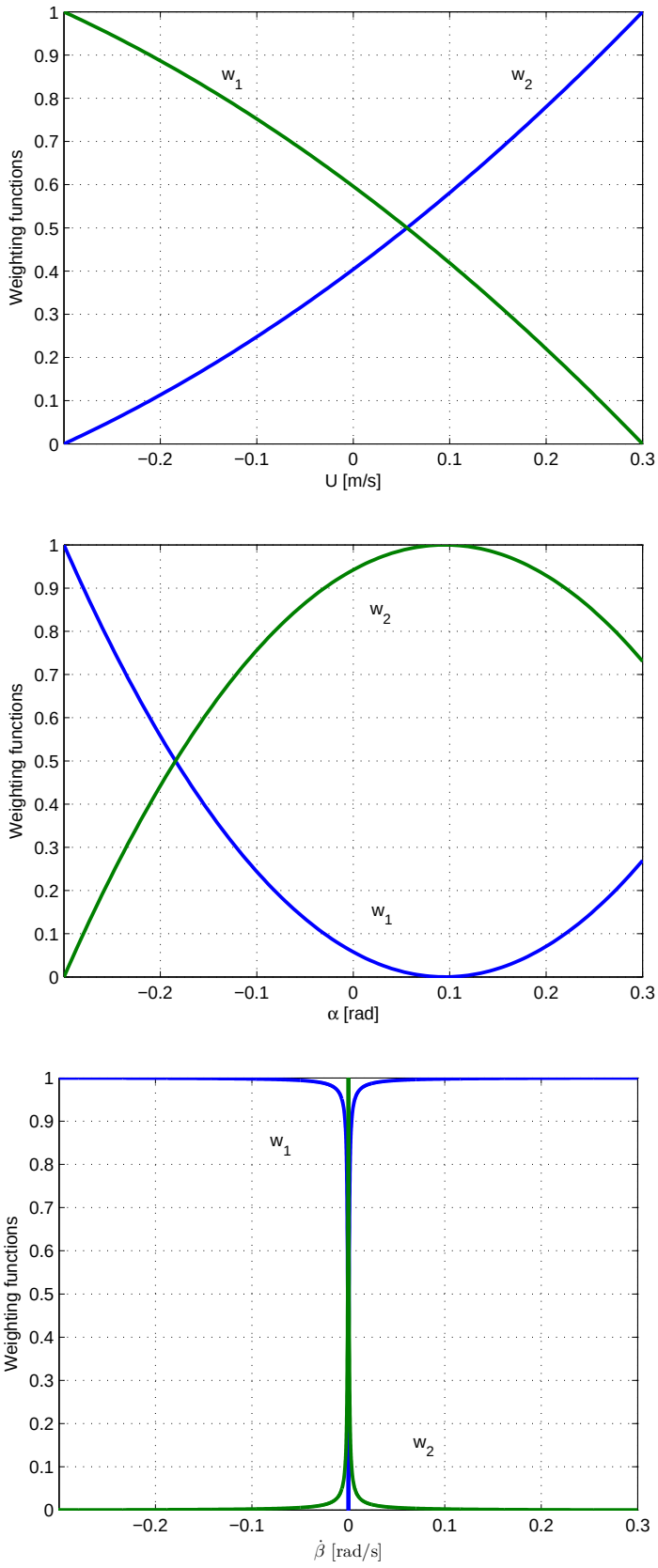

Figure 4.3: *CNO type weighting functions of the relaxed TP model for each dimension* $U[m/s]$, $\alpha[rad]$, $\dot{\beta}[rad/s]$

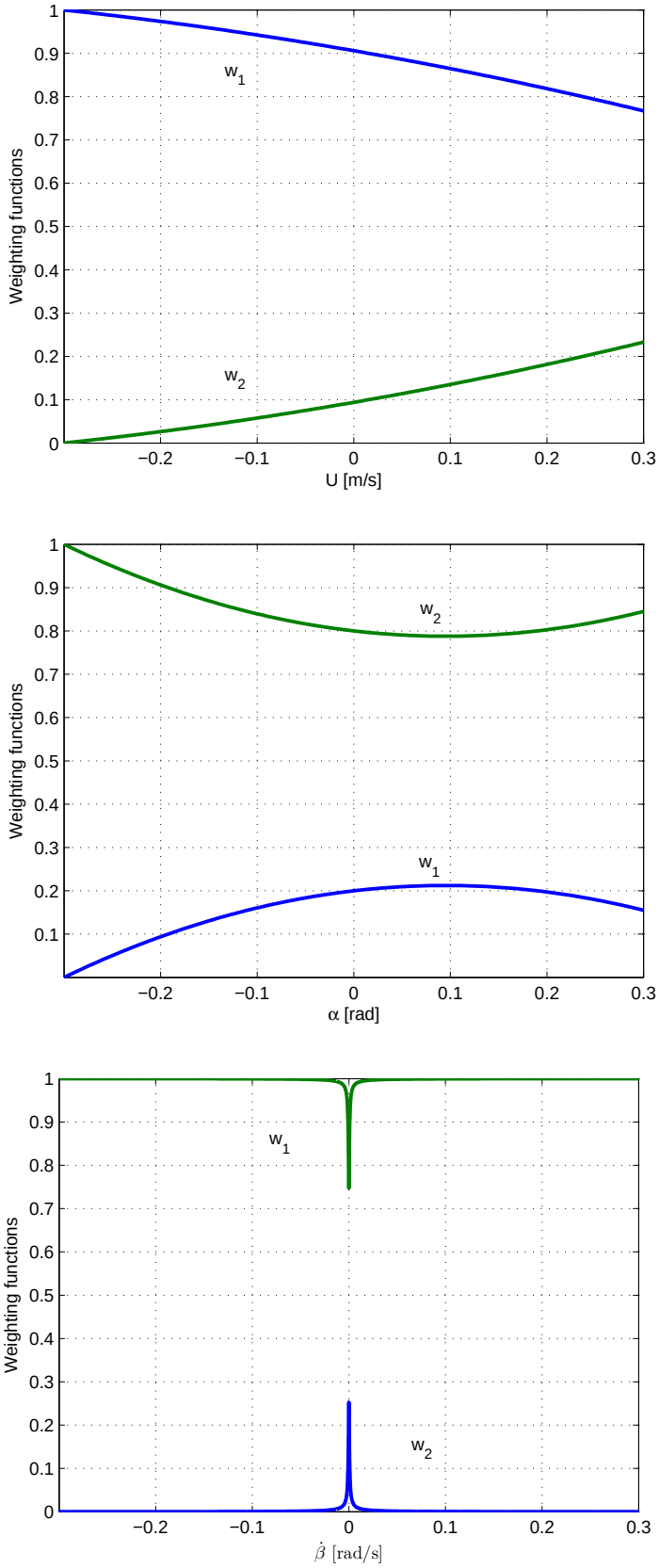

Figure 4.4: *SNNN type weighting functions of the relaxed TP model for each dimension $U[m/s]$, $\alpha[rad]$, $\dot{\beta}[rad/s]$*

with a tight (CNO: $\lambda = 100\%$) type weighting function system. Figure ?? and ?? show the weighting functions for the exact model and Figure 4.3 and 4.4 show the weighting functions for the relaxed model. This is executed both for a controller and for an observer investigation. The interpolation at both investigations is executed with the same resolution of 2% steps - in other words the value of λ is discretized over 50 points.

For each interpolation resolution point a controller and observer is designed in accordance to the LMI theorems described in Section 3.1.3, which results in 50 different controllers and 50 different observers.

4.2 Results of the 2D Analysis: Feasibility, Convexity

Figure 4.5 illustrates the relation between feasibility and convexity in case of the controller and observer design based on the exact TP model. The x-axis illustrates the convexity, namely the transition from the loose convex hull (SNNN, $\lambda = 0$) to the tight convex hull (CNO, $\lambda = 1$) corresponding to the interpolation parameter λ. The y-axis illustrates the feasibility with a line, if the LMI based design resulted in a feasible solution. The value $y = 0$ illustrates the case if the design did not yield in a feasible solution.

The controller was designed on the parameter space $U(t) = [6\ 16]$ (m/s). The results on Figure 4.5 in case of the controller show a strong correlation between the feasibility and the convexity: the feasible LMI designs appear in larger number near the tight, CNO type convex hull than the loose, SNNN type convex hull. Manipulating the interval of parameter $U(t)$ in a broad scale later in the section the same phenomenon can be seen.

The observer was designed on the parameter space $U(t) = [6\ 400]$ (m/s). The reason to select this unrealistic and large interval of the external parameter wind speed $U(t)$ is to be able to indicate the influence of the convex hull manipulation on the feasibility of the observer, which could be detected through this region, since the observer design in the interval $U(t) = [6\ 16]$ (m/s) is always feasible. The results on Figure 4.5 in case of the observer show also a relation between the feasibility and the convexity: a non feasible segment can be detected at a convex hull transitional section. Also manipulating the interval of parameter $U(t)$ in a broad scale later in the section the same phenomenon can be seen.

In this context as a conclusion of this section it can be stated that **the convexity of the polytopic TP model representation strongly influences the feasibility of LMI based designs, moreover as a further conclusion this is valid both for the controller and observer cases, in a separate, different way**.

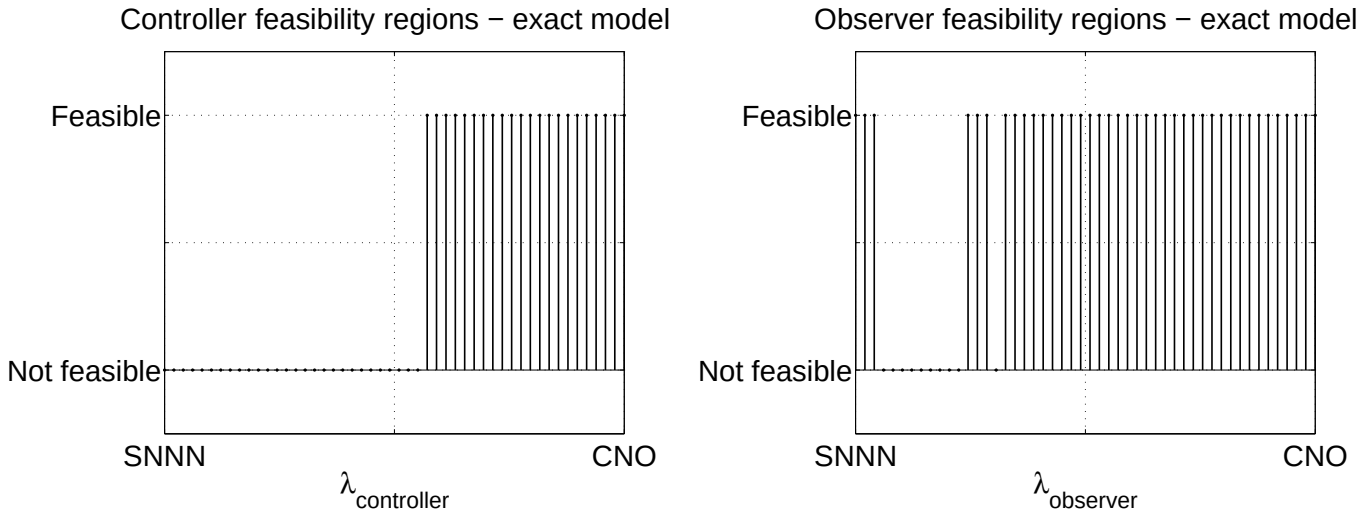

Figure 4.5: *Controller and observer feasibility regions of the exact model*

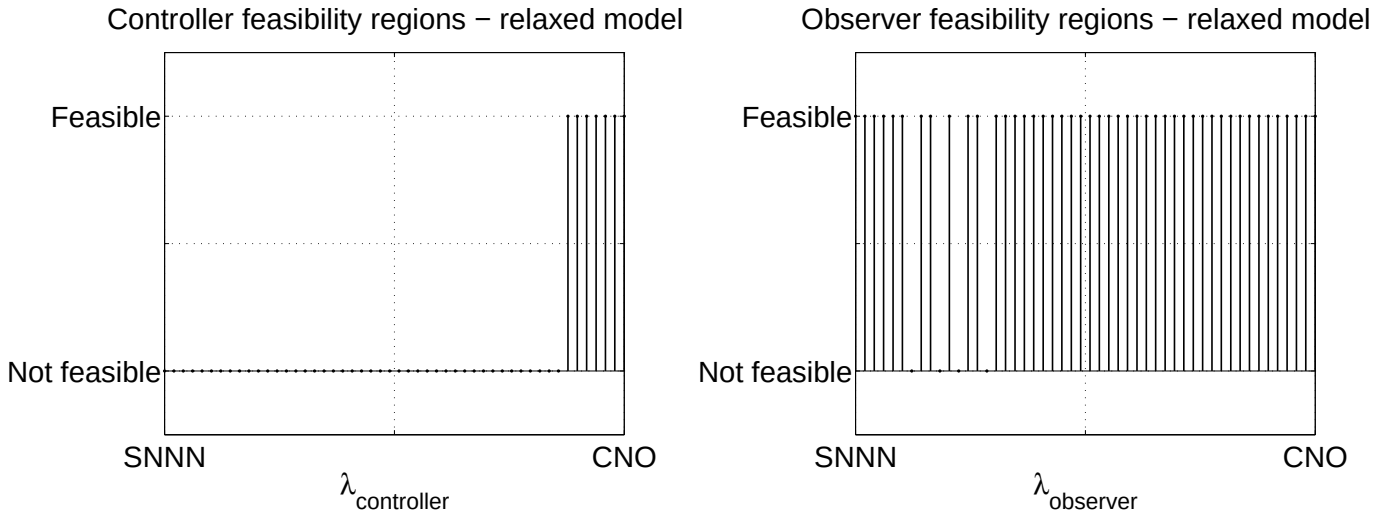

Figure 4.6: *Controller and observer feasibility regions of the relaxed model*

4.3 Results of the 3D Analysis: Feasibility, Convexity, Complexity

Figure 4.6 shows the results of the same investigation but based on the relaxed TP model. The results show that the feasibility regions are different for both the controller and observer cases from the results of the exact TP model presented in the previous section: the complexity also interferes with the feasibility. In case of the controller this region is significantly smaller. In case of the observer the feasibility region is increased in the present case.

The investigation is further continued for different intervals of the external parameter wind speed $U(t)$ and the complexity is incorporated into the graphical illustrations. As a result Figure 4.7 and 4.8 present the relation between feasibility, convexity and complexity for different intervals of parameter $U(t)$. The x-axis illustrates the convexity similarly to the previous section, the y-axis denotes the complexity of the model with the exact and relaxed TP model cases and the z-axis represents the feasibility, also similarly to the previous section. Figure 4.7 illustrates the results of the controller, with the parameter interval $U(t) = [6\ 16]$ (m/s) and $U(t) = [8\ 33]$ (m/s) and Figure 4.8 illustrates the results of the observer design with the parameter interval $U(t) = [6\ 400]$ (m/s) and $U(t) = [8\ 425]$ (m/s). The results show that the complexity of the TP model also interferes with the feasibility.

In case of the controller the feasible designs fall in number if the TP model is a relaxed model containing fewer vertexes. However, considering the convexity the feasible designs remain similarly near the tight, CNO type convex hull than the loose, SNNN type convex hull both for the relaxed and exact TP model cases.

In case of the observer the feasible designs appear in a larger number if the TP model is a relaxed model containing fewer vertexes in the present parameter interval $U(t) = [6\ 400]$ (m/s) and $U(t) = [8\ 425]$ (m/s) cases. Considering the convexity the results show similarly to the previous section a relation between the convexity and feasibility: further feasible and non feasible segments can be detected at different convex hull transitional sections.

Based on these results as a conclusion the same phenomenon can be observed as in the previous section with an additional information: **besides the convexity of the polytopic TP model representation the complexity also influences the feasibility regions of LMI based designs, moreover as a further conclusion this is valid both for the controller and observer cases, also in a separate, different way**.

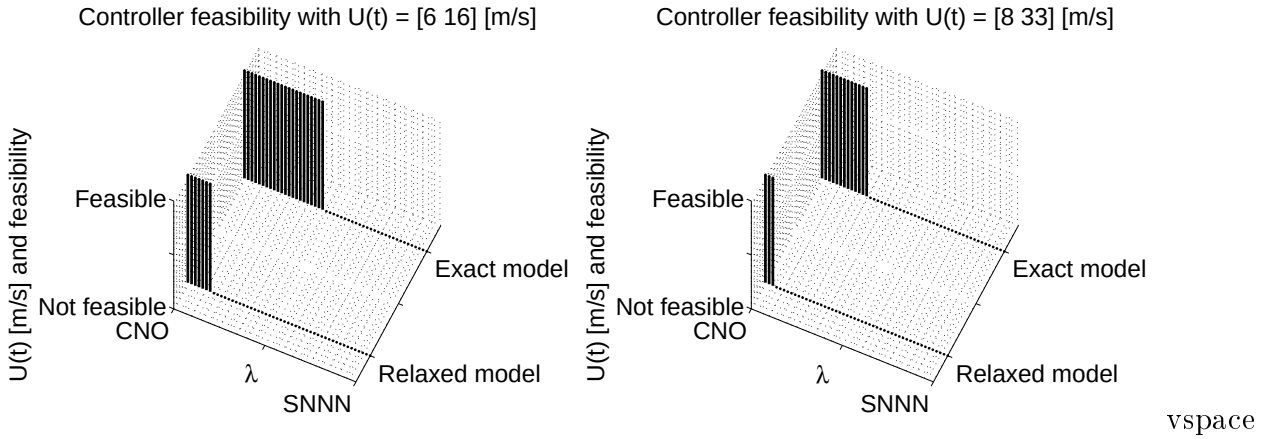

vspace

Figure 4.7: *Controller feasibility for external parameter wind speed* $U(t) = [6\ 16]\ (m/s)$ *and* $U(t) = [8\ 50]\ (m/s)$

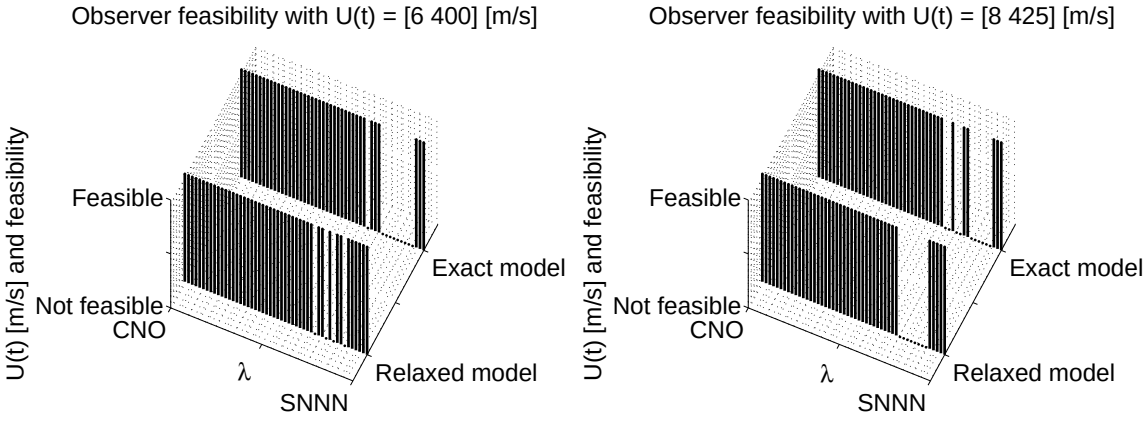

Figure 4.8: *Observer feasibility for external parameter wind speed* $U(t) = [6\ 400]\ (m/s)$ *and* $U(t) = [8\ 425]\ (m/s)$

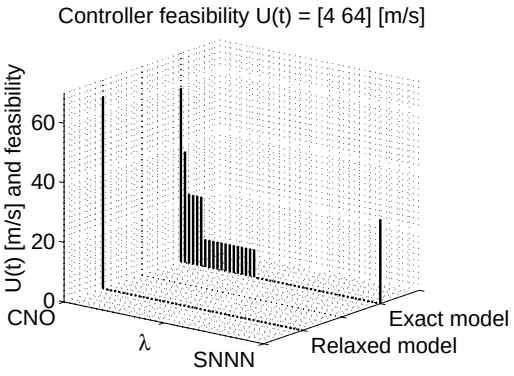

Figure 4.9: *Controller feasibility regions and achievable external parameter wind speed investigated over the interval* $U(t) \in [4\ 64]\ (m/s)$

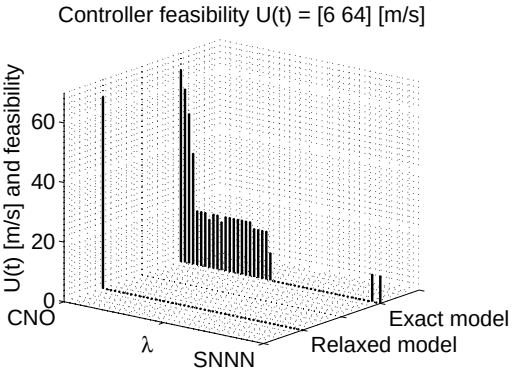

Figure 4.10: *Controller feasibility regions and achievable external parameter wind speed investigated over the interval* $U(t) \in [6\ 64]\ (m/s)$ *results*

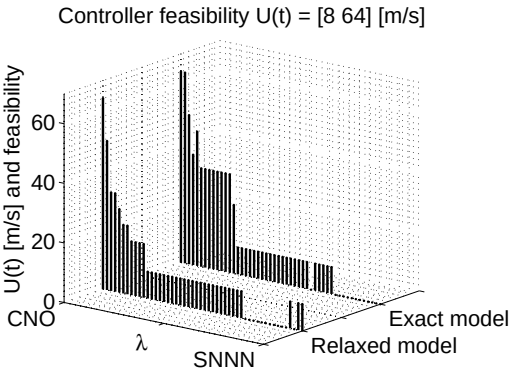

Figure 4.11: *Controller feasibility regions and achievable external parameter wind speed investigated over the interval* $U(t) \in [8\ 64]\ (m/s)$ *results*

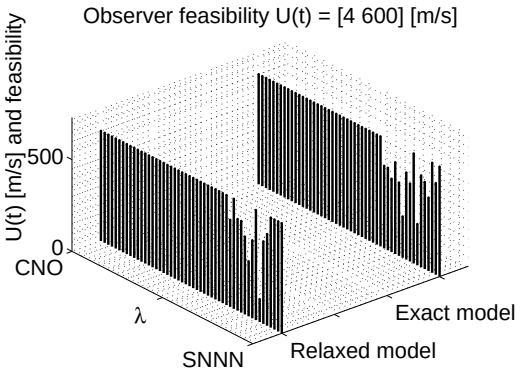

Figure 4.12: *Observer feasibility regions and achievable external parameter wind speed investigated over the interval* $U(t) \in [4\ 600]\ (m/s)$

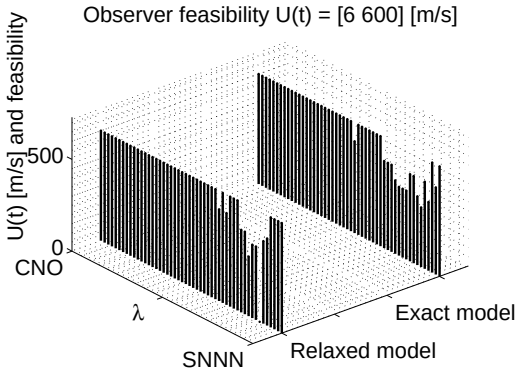

Figure 4.13: *Observer feasibility regions and achievable external parameter wind speed investigated over the interval* $U(t) \in [6\ 600]\ (m/s)$

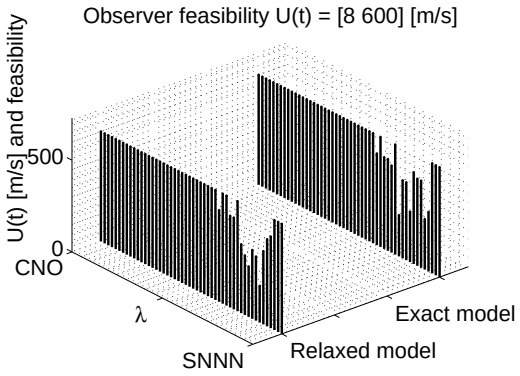

Figure 4.14: *Observer feasibility regions and achievable external parameter wind speed investigated over the interval* $U(t) \in [8\ 600]\ (m/s)$

4.4 Results of the 4D Analysis: Feasibility, Convexity, Complexity, Parameter space

Continuing the investigation further and incorporating the parameter space into the graphical illustrations as a result the figures 4.9-4.11 and 4.12-4.14 illustrate the relation between feasibility, convexity, complexity and the parameter space with the external parameter wind speed $U(t)$. The axes of the figures are the same as on the figures of the previous sections, the difference is that the z-axis provides additional information about the external parameter wind speed $U(t)$, namely it also illustrates the maximal achievable value U_{max} of the interval: a line denotes if the LMI based design is feasible and the height indicates the value of U_{max}. Figures 4.9-4.11 illustrate the case of the controller with the the parameter intervals $U(t) \in [4\ 64]\ (m/s)$, $U(t) \in [6\ 64]\ (m/s)$ and $U(t) \in [8\ 64]\ (m/s)$ and Figures 4.12-4.14 illustrate the case of the observer with the the parameter intervals $U(t) \in [4\ 600]\ (m/s)$, $U(t) \in [6\ 600]\ (m/s)$ and $U(t) \in [8\ 600]\ (m/s)$. The investigation was executed in an iterative manner: an LMI based design is executed for the current value U_{max} of the parameter interval and the feasibility of the design is checked. If the design is feasible, the maximal value U_{max} of the interval is increased, the LMI based design is repeated and the feasibility is checked. This is executed until the design is still feasible. The results show that the size of the parameter space of the TP model also interferes with the feasibility.

It can be seen in case of the controller that the previously stated phenomenons considering convexity and complexity are also valid, with an additional statement: the feasible designs fall in number if the TP model is a relaxed model containing fewer vertexes, the feasible LMI designs appear in larger number near the tight, CNO type convex hull, but the feasible results also appear with a higher achievable parameter interval value U_{max} near the tight, CNO type convex hull. In case of the controller the achievable parameter interval value U_{max} reaches the value of $64\ (m/s)$ at the tight, CNO type convex hull, whereas it only reaches a smaller value at the transitional cases further from the tight, CNO type convex hull.

In case of the observer it can be determined that the relation between the convexity and feasibility show a similarity to the previous section: feasible and non feasible segments can be detected at different convex hull transitional sections. Considering the complexity the feasible designs appear not necessarily in a larger number if the TP model is a relaxed model containing fewer vertexes but nevertheless a difference in the feasibility regions can be detected between the exact and relaxed TP model cases. Lastly, examining from the parameter space's point of view instead of a peak seen at the controller's case in case of the observer rather a crater/pit/hole can be

detected in the feasibility sections.

In this context as a conclusion the following can be stated: **the convexity and complexity of the polytopic TP model representation strongly influences the feasibility regions of LMI based designs in a different way for controller and observer, and it also has a strong effect on the achievable external parameter wind speed U_{max} where the LMI based design is feasible**.

Chapter 5

Conclusion

The Scientific Student Conference paper presented the systematic method which was developed and executed for investigating the hypothesis, its proving results and consequences which lead to the proof of the hypothesis based on the control design example of a quasi Linear Parameter Varying (qLPV) state-space model. The results illustrate that the manipulation of the vertexes of the polytopic Tensor Product (TP) model representation strongly influences the feasibility of the Linear Matrix Inequality (LMI) based control design. The attributes of the vertexes' influencing the feasibility regions of the LMI based controller and observer design include the position and the number of the vertexes contained in the polytopic model. This confirms the necessity and importance of the polytopic manipulation, namely the fact that the LMI based control design methods do not give an optimal solution on the identified qLPV model but rather on the polytopic representation. Furthermore the paper shows that the vertexes of the polytopic TP model representation also influence the size of the achievable parameter space where the LMI based design is feasible. These statements have been proved valid both for the feasibility of the controller's and the observer's LMI based design, but the influence differs in its characteristics for the controller and the observer system components.

The proved statements and the regarding concepts gain further new research directions in the field of qLPV and LMI based control theory research.

Regarding future work one goal includes the further investigation of the effect of the polytopic manipulation on the control performance, which may further expand the statement.

References

[1] J. Shamma and M. Athans, "Guaranteed properties of gain scheduled control for linear parameter-varying plants," *Automatica*, vol. 27, no. 3, pp. 559–564, 1991.

[2] M. Athans, S. Fekri, and A. Pascoal, "Issues on robust adaptive feedback control," in *Proceedings of 16th IFAC world congress, Prague, Czech Republic*, 2005, pp. 9–39.

[3] J. Hespanha, D. Liberzon, and A. Morse, "Overcoming the limitations of adaptive control by means of logic-based switching," *Systems & Control Letters*, vol. 49, no. 1, pp. 49–65, 2003.

[4] G. Feng and J. Ma, "Quadratic stabilization of uncertain discrete-time fuzzy dynamic systems," *Circuits and Systems I: Fundamental Theory and Applications, IEEE Transactions on*, vol. 48, no. 11, pp. 1337–1344, 2001.

[5] M. Ravindranathan and R. Leitch, "Model switching in intelligent control systems," *Artificial intelligence in engineering*, vol. 13, no. 2, pp. 175–187, 1999.

[6] P. Apkarian and P. Gahinet, "A convex characterization of gain-scheduled H_∞ controllers," *IEEE Transactions on Automatic Control*, vol. 40, no. 5, pp. 853–864, 1995.

[7] P. Gahinet, "Explicit controller formulas for LMI-based H_∞ synthesis," in *Proceedings of the 1994 American Control Conference*, vol. 3, Baltimore, Maryland, USA, 1994, pp. 2396–2400.

[8] P. Gahinet and A. Laub, "Reliable computation of γ_{opt} in singular H_∞ control," in *Proceedings of the 33rd IEEE Conference on Decision and Control, 1994*, vol. 2, Orlando, Florida, USA, 1994, pp. 1527–1532.

[9] I. Kaminer, P. Khargonekar, and M. Rotea, "Mixed H_2/H_∞ control for discrete-time systems via convex optimization," *Automatica*, vol. 29, no. 1, pp. 57–70, 1993.

[10] S. Boyd, L. E. Ghaoui, E. Feron, and V. Balakrishnan, *Linear Matrix Inequalities in Systems and Control Theory*. Society for Industrial Mathematics, 1994, vol. 15.

[11] J. Bokor and G. Balas, "Linear matrix inequalities in systems and control theory," *Preprints 16th IFAC World Congress*, 2005, p. Keynote lecture.

[12] Y. Nesterov and A. Nemirovskii, *Interior-point polynomial algorithms in convex programming*. SIAM Studies in Applied Mathematics, 1994.

[13] I. Grattan-Guinness, "A sideways look at Hilbert's twenty-three problems of 1900," *Notices of the AMS*, vol. 47, no. 7, pp. 752–757, 2000.

[14] J. Gray, "The Hilbert problems 1900-2000," *Newsletter*, vol. 36, no. 10-13, pp. 1–1, 2000.

[15] D. Hilbert, "Mathematische probleme," *2nd International Congress of Mathematican*, 1900, paris, France.

[16] I. Kaplansky, *Hilbert's problems*. University of Chicago, 1977.

[17] V. Arnold, "On functions of three variables," *Doklady Akademii Nauk SSSR*, vol. 114, no. 4, pp. 679–681, 1957.

[18] A. Kolmogorov, "On the representation of continuous functions of many variables by superposition of continuous functions of one variable and addition," in *Doklady Akademii Nauk SSSR*, vol. 114, 1957, pp. 953–956.

[19] D. Sprecher, "On the structure of continuous functions of several variables," *Transactions of the American Mathematical Society*, vol. 115, pp. 340–355, 1965.

[20] G. Lorentz, *Approximation of functions*. Holt, Rinehart and Winston (New York), 1966.

[21] G. Cybenko, "Approximation by superpositions of a sigmoidal function," *Mathematics of Control, Signals, and Systems (MCSS)*, vol. 2, no. 4, pp. 303–314, 1989.

[22] K. Hornik, M. Stinchcombe, and H. White, "Multilayer feedforward networks are universal approximators," *Neural networks*, vol. 2, no. 5, pp. 359–366, 1989.

[23] J. Castro, "Fuzzy logic controllers are universal approximators," *IEEE Transactions on Systems, Man and Cybernetics*, vol. 25, no. 4, pp. 629–635, 1995.

[24] B. Kosko, "Fuzzy systems as universal approximators," in *Proceedings of the 1st IEEE International Conference on Fuzzy Systems, 1992*, San Diego, California, USA, 1992, pp. 1153–1162.

[25] G. Stewart, "On the early history of singular value decomposition," Institute for Advanced Computer Studies, University of Maryland, Tech. Rep. TR–92–31, March 1992.

[26] G. Golub and W. Kahan, "Calculating the singular values and pseudo-inverse of a matrix," *Journal of the Society for Industrial and Applied Mathematics: Series B, Numerical Analysis*, pp. 205–224, 1965.

[27] G. Golub and C. Reinsch, "Singular value decomposition and least squares solutions," *Numerische Mathematik*, vol. 14, no. 5, pp. 403–420, 1970.

[28] G. Golub and C. Reinsch, "Singular value decomposition and least squares solutions," *Handbook for Automatic Computation Die Grundlehren der mathematischen Wissenschaften*, vol. 186, pp. 134–151, 1971.

[29] E. Deprettere, *SVD and signal processing: algorithms, applications and architectures*. Amsterdam, The Netherlands: North-Holland Publishing Co., 1988.

[30] R. Vaccaro, *SVD and Signal Processing II: Algorithms, analysis and applications*. Elsevier Science, 1991.

[31] M. Moonen and B. De Moor, *SVD and signal processing III: algorithms, architectures, and applications*. Elsevier Science, 1995.

[32] M. Petrou and C. Petrou, *Image Processing: The Fundamentals*. Wiley, 2010.

[33] S. Banerjee and A. Roy, *Linear Algebra and Matrix Analysis for Statistics*. Chapman and Hall, CRC, 2014.

[34] L. De Lathauwer, B. De Moor, and J. Vandewalle, "A multilinear singular value decomposition," *SIAM Journal on Matrix Analysis and Applications*, vol. 21, no. 4, pp. 1253–1278, 2000.

[35] Y. Yam, "Fuzzy approximation via grid point sampling and singular value decomposition," *IEEE Transactions on Systems, Man, and Cybernetics, Part B: Cybernetics*, vol. 27, no. 6, pp. 933–951, 1997.

[36] Y. Yam, P. Baranyi, and C. Yang, "Reduction of fuzzy rule base via singular value decomposition," *IEEE Transactions on Fuzzy Systems*, vol. 7, no. 2, pp. 120–132, 1999.

[37] L. De Lathauwer, B. De Moor, and J. Vandewalle, "Blind source separation by higher order singular value decomposition," in *Proceedings of the European Signal Processing Conference, 1994*, vol. 1, Edinburgh, Scotland, UK, 1994, pp. 175–178.

[38] L. De Lathauwer, "Signal processing based on multilinear algebra," Ph.D. dissertation, Katholieke Universiteit Leuven, Belgium, 1997.

[39] P. Baranyi, L. Szeidl, P. Várlaki, and Y. Yam, "Definition of the HOSVD based canonical form of polytopic dynamic models," in *Proceedings of the 2006 IEEE International Conference on Mechatronics*, Budapest, Hungary, July 3-5 2006, pp. 660–665.

[40] P. Baranyi, L. Szeidl, and P. Várlaki, "Numerical reconstruction of the HOSVD based canonical form of polytopic dynamic models," in *Proceedings of the 10th International Conference on Intelligent Engineering Systems, 2006*, London, UK, June 26-28 2006, pp. 196–201.

[41] L. Szeidl and P. Várlaki, "HOSVD based canonical form for polytopic models of dynamic systems," *Journal of Advanced Computational Intelligence and Intelligent Informatics*, vol. 13, no. 1, pp. 52–60, 2009.

[42] P. Baranyi, Y. Yam, and P. Varlaki, *Tensor product model transformation in polytopic model-based control.* Boca Raton, Fla.; London: CRC; Taylor & Francis [distributor], 2010.

[43] P. Baranyi, D. Tikk, Y. Yam, and R. Patton, "From differential equations to PDC controller design via numerical transformation," *Computers in Industry*, vol. 51, no. 3, pp. 281–297, 2003.

[44] P. Baranyi, "TP model transformation as a way to LMI-based controller design," *IEEE Transactions on Industrial Electronics*, vol. 51, no. 2, pp. 387–400, 2004.

[45] P. Baranyi, "The Generalized TP Model Transformation for T-S Fuzzy Model Manipulation and Generalized Stability Verification," *IEEE Transactions on Fuzzy Systems*, vol. 22, no. 4, 2013.

[46] P. Baranyi, Z. Petres, P. Korondi, Y. Yam, and H. Hashimoto, "Complexity relaxation of the tensor product model transformation for higher dimensional problems," *Asian Journal of Control*, vol. 9, no. 2, pp. 195–200, 2007.

[47] Z. Petres, P. Baranyi, and H. Hashimoto, "Approximation and complexity tradeoff by TP model transformation in controller design: A case study of the TORA system," *Asian Journal of Control*, vol. 12, no. 5, pp. 575–585, 2010.

[48] P. Baranyi, "Convex hull generation methods for polytopic representations of lpv models," *Proc. of the 7th International Symposium on Applied Machine Intelligence and Informatics (SAMI 2009)*, pp. 69–74, 2009.

[49] D. Tikk, P. Baranyi, and R. Patton, "Approximation properties of TP model forms and its consequences to TPDC design framework," *Asian Journal of Control*, vol. 9, no. 3, pp. 221–231, 2007.

[50] K. Tanaka and H. Wang, *Fuzzy control systems design and analysis: a linear matrix inequality approach.* Wiley-Interscience, 2001.

[51] C. Scherer and S. Weiland, "Linear matrix inequalities in control," *Lecture Notes, Dutch Institute for Systems and Control, Delft, The Netherlands*, 2000, http://www.cs.ele.tue.nl/sweiland/lmi.htm.

[52] B. Takarics and P. Baranyi, "Tensor-product-model-based control of a three degrees-of-freedom aeroelastic model," *Journal of Guidance, Control, and Dynamics*, vol. 36, no. 5, pp. 1527–1533, 2013.

[53] V. Mukhopadhyay, "Historical perspective on analysis and control of aeroelastic responses," *Journal of Guidance, Control, and Dynamics*, vol. 26, no. 5, pp. 673–684, 2003.

[54] Z. Prime, B. Cazzolato, C. Doolan, and T. Strganac, "Linear-parameter-varying control of an improved three-degree-of-freedom aeroelastic model," *Journal of Guidance, Control and Dynamics*, vol. 33, no. 2, pp. 615–619, 2010.

[55] J. Block and H. Gilliatt, "Active control of an aeroelastic structure," Master's thesis, Texas A&M University, 1996.

[56] J. Block and T. Strganac, "Applied active control for a nonlinear aeroelastic structure," *Journal of Guidance, Control, and Dynamics*, vol. 21, no. 6, pp. 838–845, 1998.

[57] V. Mukhopadhyay, "Transonic flutter suppression control law design and wind-tunnel test results," *Journal of Guidance, Navigation, and Control*, vol. 23, no. 5, pp. 930–937, 2000.

[58] T. W. Strganac, J. Ko, and D. E. Thompson, "Identification and control of limit cycle oscillations in aeroelastic systems," *Journal of Guidance, Control, and Dynamics*, vol. 23, no. 6, pp. 1127–1133, 2000.

[59] S. N. Singh and L. Wang, "Output feedback form and adaptive stabilization of a nonlinear aeroelastic system," *Journal of Guidance, Control, and Dynamics*, vol. 25, no. 4, pp. 725–732, 2002.

[60] G. Platanitis and T. Strganac, "Supression of control reversal using leading- and trailing-edge control surfaces," *Journal of Guidance, Control, and Dynamics*, vol. 28, no. 3, pp. 452–460, 2005.

[61] K. Reddy, K. Chen, A. Behal, and P. Marzocca, "Multi-input/multi-output adaptive output feedback control design for aeroelastic vibration suppression," *Journal of Guidance, Control, and Dynamics*, vol. 30, no. 4, pp. 1040–1048, 2007.

[62] P. Baranyi, "Tensor-product model-based control of two-dimensional aeroelastic system," *Journal of Guidance, Control, and Dynamics*, vol. 29, no. 2, pp. 391–400, 2006.

[63] P. Baranyi, "Output feedback control of two-dimensional aeroelastic system," *Journal of Guidance, Control and Dynamics*, vol. 29, no. 3, pp. 762–767, 2006.

[64] Z. Prime, B. Cazzolato, and C. Doolan, "A mixed H_2/H_∞ scheduling control scheme for a two degree-of-freedom aeroelastic system under varying airspeed and gust conditions," in *Proceedings of the AIAA Guidance, Navigation and Control Conference*, Honolulu, Hawaii, USA, 2008, pp. 18–21.

[65] K. W. Lee and S. N. Singh, "Multi-input noncertainty-equivalent adaptive control of an aeroelastic system," *Journal of Guidance, Control, and Dynamics*, vol. 33, no. 5, pp. 1451–1460, 2010.

[66] S. Singh and S. Gujjula, "Variable structure control of unsteady aeroelastic system with partial state information," *Journal of Guidance, Control and Dynamics*, vol. 28, no. 3, pp. 568–573, 2005.

[67] C. Lin and W. Chin, "Adaptive decoupled fuzzy sliding-mode control of a nonlinear aeroelastic system," *Journal of Guidance, Control and Dynamics*, vol. 29, no. 1, pp. 206–209, 2006.

[68] N. Bhoir and S. Singh, "Control of unsteady aeroelastic system via state-dependent riccati equation method," *Journal of Guidance, Control and Dynamics*, vol. 28, no. 1, pp. 78–84, 2005.

[69] K. Lee and S. Singh, "Global robust control of an aeroelastic system using output feedback," *Journal of Guidance, Control and Dynamics*, vol. 30, no. 1, pp. 271–275, 2007.

[70] S. SINGH and M. Brenner, "Modular adaptive control of a nonlinear aeroelastic system," *Journal of Guidance, Control and Dynamics*, vol. 26, no. 3, pp. 443–451, 2003.

[71] W. Xing and S. Singh, "Adaptive output feedback control of a nonlinear aeroelastic structure," *Journal of Guidance, Control and Dynamics*, vol. 23, no. 6, pp. 1109–1116, 2000.

[72] M. Waszak, "Robust multivariable flutter suppression for the benchmark active control technology (BACT) wind-tunnel model," *Journal of Guidance, Control, and Dynamics*, vol. 24, no. 1, pp. 147–143, 1997.

[73] R. Scott and L. Pado, "Active control of wind-tunnel model aeroelastic response using neural networks," *Journal of Guidance, Control and Dynamics*, vol. 23, no. 6, pp. 1100–1108, 2000.

[74] J. Ko, T. Strganac, and A. Kurdila, "Stability and control of a structurally nonlinear aeroelastic system," *Journal of Guidance, Control and Dynamics*, vol. 21, pp. 718–725, 1998.

[75] J. Ko, A. Kurdila, and T. Strganac, "Nonlinear control of a prototypical wing section with torsional nonlinearity," *Journal of Guidance, Control and Dynamics*, vol. 20, no. 6, pp. 1180–1189, 1997.

[76] S. Joshi and A. Kelkar, "Passivity-based robust control with application to benchmark active controls technology wing," *Journal of Guidance, Control and Dynamics*, vol. 23, no. 5, pp. 938–947, 2000.

[77] P. Baranyi and B. Takarics, "Aeroelastic wing section control via relaxed tensor product model transformation framework," *Journal of Guidance, Control, and Dynamics*, vol. 36, no. 5, pp. 1527–1533, 2013.

Appendix

A.1 Acronyms

The following abbreviations are used in the paper:

LPV	Linear Parameter Varying
qLPV	quasi Linear Parameter Varying
LTI	Linear Time Invariant
LMI	Linear Matrix Inequality
SVD	Singular Value Decomposition
HOSVD	Higher-Order Singular Value Decomposition
ICA	Independent Component Analysis
TP model	Tensor Product model
CNO	Close to Normal
SNNN	Sum-Normalized Non-Negative
NATA	Nonlinear Aeroelastic Test Apparatus
DoF	Degree of Freedom